ResearchGate

See discussions, stats, and author profiles for this publication at: https://www.researchgate.net/publication/233495112

A Proposal for a Minimal Model of Free Reeds

Article *in* Acta Acustica united with Acustica · January 2007

CITATIONS
12

READS
790

2 authors, including:

Laurent Millot
Ecole Nationale Supérieure Louis-Lumière

30 PUBLICATIONS **42** CITATIONS

SEE PROFILE

Some of the authors of this publication are also working on these related projects:

Physics of free reeds instruments: from modeling to numerical simulation View project

Second release for IDS Analysis Tools - Mac OS 10.15 an Windows 10 View project

All content following this page was uploaded by Laurent Millot on 03 October 2016.

The user has requested enhancement of the downloaded file.

A proposal for a minimal model of free reeds

L. Millot, Cl. Baumann
l.millot@ens-louis-lumiere.fr

Abstract

In this paper we propose a minimal model for free reeds taking into account the significant phenomena. This free reed model may be used to build models of free reed instruments which permit numerical simulations. Several definitions for the section by which the airflow passes through the reed are reviewed and a new one is proposed which takes into account the entire escape area under the reed and the reed thickness. To derive this section, it is necessary to distinguish the neutral section (the only section of the reed which always keeps its length constant while moving) from the upstream or downstream sections. A minimal configuration is chosen to permit the instabilities of both (-,+) and (+,-) reeds on the basis of a linear analysis of instabilities conditions. This configuration is used to illustrate, with temporal simulations, the minimal model for both kinds of reeds and to discuss the model assumptions. Some clues are given about the influence, on the playing frequency and on the dynamic of the sound, of two main parameters of the geometrical model: the size of the volume and the level of the excitation. It is shown that the playing frequency of a (+,-) reed can vary in a large range according to the size of the volume upstream of the reed; that the playing frequency is nearly independent of the excitation but that the dynamic of the sound increases with the excitation level. Some clues are also proposed to determine the nature of the bifurcation for free reeds: it seems that free reeds may present inverse bifurcations. The influence of the reed thickness is also studied for configurations where the reed length or the reed width vary to keep the mass constant. This study shows that the reed thickness can have a great influence on the sound magnitude, the playing frequency and the magnitude of the reed displacement which justifies its introduction in the reed model.

This article has been published in Acta Acustica united with Acustica, Vol. 93 (2007), p. 122-144.

1 Introduction

Since the first works of Helmholtz [1], much attention has been paid to the study of reeds and reeds instruments. One can find a great deal of works related to striking reed auto-oscillation [2, 3, 4, 5, 6, 7, 8, 9, 10] and synthesis of the clarinet or saxophone [11, 12, 13, 14] for instance. But there are far less works related to free reeds dynamics [15, 16, 17, 18, 19] and most of the articles dealing with modelling of free reeds are only

concerned with frequency-domain approach and the threshold of reed auto-oscillation [20, 21, 22, 23, 24, 25, 26, 27, 28]. To have an idea of most of the latest available information on free-reed modelling, the reader is invited to search in [29]. We adopt Fletcher's convention [25, 29] to designate both kinds of reed: (-,+) for an blown closed reed and (+,-) for a blown open reed.

A first attempt to obtain a temporal model for a free-reed is due to St-Hilaire, Wilson and Beavers [30]. In this paper, a three-dimensional farfield flow is matched with a two-dimensional near field one. Since this first attempt, Van Hassel and Hirschberg [31] have shown that it would not be more difficult to solve the three-dimensional problem rather than using a 2D/3D matching which is rather arbitrary. Some new research on the 3D modelling seem to be on the way [32, 33].

To derive a satisfactory model for the free reed we already have some key information about the behaviour of the free reeds. Indeed, it has been shown [18, 34, 35] that the reed motion is almost perfectly sinusoidal during playing because of the non-striking nature of the reeds. Another experiment made by Misdariis, Ricot and Caussé [32, 36] using a laser vibrometer confirmed the sinusoidal character of free reed motion.

The present research is a proposal of a model which may be used to obtain time simulation of the instrument useful for sound synthesis and comparison with measurements. While the model is globally one-dimensional, the description of the flow through the reed takes into account the side and front escape areas under both reeds. In section 2, we first point out some ambiguities concerning the description of the reed motion. Then we complete the free reed model by discussing the definition of the total volume flow which passes through the reed, by taking into account the local longitudinal and transverse deformations of the reed. In section 3, we first introduce a minimal loading configuration which may permit the instabilities of both kinds of reed: (-,+) and (+,-) reeds. The conditions for the instability of both kinds of reed are derived according to a linear analysis. We then illustrate the model for both kinds of reed and discuss the validity of the assumptions. Then, some preliminary results are given about the influence of some main control parameters: the excitation, the size of the volume upstream of the reed and the reed thickness. Some clues about the nature of the bifurcation in the case of free reeds are also given. In the Appendix, one can find the details for the derivation of the motion of the different reed sections, for the pumped volume flow, for the calculation of the instability condition and some keypoints about the algorithm we used to perform numerical simulations.

We must emphasise that this study has not been confronted with experiments for the moment in the case of the configurations we used: only numerical simulations are used to illustrate the model we propose. But this free reed model has been successfully used for the study of chromatic playing on a diatonic harmonica, which will be presented elsewhere.

2 Reed minimal model

2.1 Description of the reed motion

As demonstrated by Millot [34, 35] using strain gauges, Ricot [36] or Cottingham [18] using a laser vibrometer, the reed motion is sinusoidal for a free reed: each reed is moving on the first transverse eigenmode of a free-clamped beam, the Euler-Bernoulli assumption for the beams. So, to derive our model, we only consider pure flexion motion of the reed on its first transverse mode, which means that the cross sections of the reed are assumed to stay normal to the neutral section, the only section which does not suffer from compression or extension. In the following, we call respectively upstream and downstream sections, the faces of the reeds inside and outside of the instruments as illustrated by Figure 1. We then assume that the target face is the upstream one for the (-,+) reed and the downstream one for the (+,-) reed, using the conventions proposed by Fletcher [21].

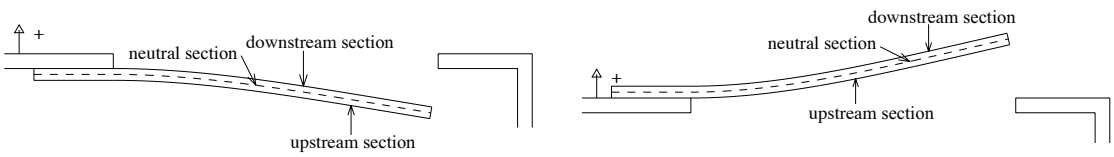

Figure 1: Definition of upstream and downstream sections for the two types of reeds which will be studied: (-,+) reed on the left and (+,-) reed on the right. The upstream section is related to the face which is in front of the inside of the instrument while the downstream section faces the outside of the instrument. The introduction of these two sections will be useful to define the output sections for the airflow.

Table 1 gives all the conventions used for the model.

The reed motion can be described by considering an equivalent mass-spring-damper oscillator with a single degree of freedom, the neutral section transverse displacement at the free tip of the reed, which will be noted h_n in the following. In almost all the former works dealing with the dynamics of reeds [37, 2, 38, 21, 12, 39, 40, 25, 41, 14, 34, 36, 28], the equivalent reed motion equation, which is normally only valid for the neutral section, is used for the upstream or downstream section following the assumption that this is a fair approach as the reeds are quite thin. For the derivation of our model, we can not afford such a simplification as we need to distinguish neutral, upstream and downstream sections and because we think that the reed thickness can not be neglected.

The respective expressions for the transverse local displacement at the distance $s.L_r$ from the clamped end ($s \in [0, 1]$), of the neutral, upstream and downstream sections are respectively for a (-,+) reed:

$$h_n(s) = h_{n,000} + \big(h_n - h_{n,000}\big)\psi(s) \tag{1}$$

symbol	related quantity
L_r	length of the reed
W_r	width of the reed
e_r	thickness of the reed
e_s	thickness of the support
s	normalised distance from the clamped end of the reed
h_{min}	clearance gap existing between the reed and the support
h_n	transverse displacement of the neutral section at the free tip of the reed
h_{up}	transverse displacement of the upstream section at the free tip of the reed
h_{do}	transverse displacement of the downstream section at the free tip of the reed
$h_{n,0}$	mean value for h_n during the oscillation
$h_{n,00}$	rest value for h_n when the reed is unblown
$h_{n,000}$	value of h_n for which the reed is flat
$h_n(s)$	transverse displacement of the neutral section at position $s.L_r$
$h_{up}(s)$	transverse displacement of the upstream section at position $s.L_r$
$h_{do}(s)$	transverse displacement of the downstream section at position $s.L_r$
$\psi(s)$	normalised modal reed factor for the first transverse eigen mode
ζ	equilibrium displacement at the free tip: $\zeta = h_n - h_{n,00}$
Δp	pressure difference between the upstream and downstream of the reed

Table 1: Definition of the symbols introduced for the reed description.

$$h_{up}(s) = h_n(s) - \frac{e_r}{2}\frac{L_r}{\sqrt{L_r^2 + (h_n - h_{n,000})^2\psi'(s)^2}} \tag{2}$$

$$h_{do}(s) = h_n(s) + \frac{e_r}{2}\frac{L_r}{\sqrt{L_r^2 + (h_n - h_{n,000})^2\psi'(s)^2}} \tag{3}$$

where $h_{n,000} = -e_s - \frac{e_r}{2}$ represents the transverse position of the neutral section when the reed is flat and $\psi(s)$ is the modal reed factor at the distance $s.L_r$ from the clamped end. It is then obvious that the upstream, downstream and neutral transverse displacements differences are greater as much as e_r, L_r and h_n increase.

We consider that the equivalent reed motion equation is a function of the neutral section equilibrium displacement at the free tip of the reed, $\zeta = h_n - h_{n,00}$, where $h_{n,00}$ is the neutral section transverse position at rest (we assume that the reed adopts a first eigenmode profile at rest). This motion equation is then given by:

$$\frac{d^2\zeta}{dt^2} + Q^{-1}\omega_0\frac{d\zeta}{dt} + \omega_0^2\zeta = \mu\Delta p \tag{4}$$

where Δp is the pressure difference between the upstream and the downstream of the reed (see Appendix for the analytical calculation of parameter μ).

As the reed motion equation is defined, we now need to consider the description of the volume flow passing through the reed.

2.2 Airflow through the reed

Following Thompson [38], Hirschberg [41] and Gazengel [14], the first component of the output flow to consider, noted u_p, is the volume flow induced by the motion of the reed (the "pumped" flow) whose expression is:

$$u_p(t) = S_r \frac{d\zeta}{dt} \tag{5}$$

As explained in the Appendix, the effective section introduced by the calculation of u_p is equal to the effective section associated with the over-pressure Δp in the reed motion equation.

The second contribution to the output flow is the flow passing under the reed. This flow is noted u_t and its expression is:

$$u_t(t) = \alpha.S_u(h_n).v_j \tag{6}$$

where α is the *vena contracta* coefficient, v_j the velocity inside the free jet and S_u the useful section whose definition will be discussed in the next section. We also assume that the jet velocity is the same in the whole jet even if the jet sheds all around the reed. This assumption may be a point of improvement for the proposed model but, in this case, a three dimensional description of the flow through the reed may be needed which is out of purpose here. As the reed scales are tiny compared to the wavelengths, we think that considering the same velocity and over-pressure all over the reed is a fair first approach.

To complete the description of the airflow through the reed, we need to introduce a relation between the jet velocity v_j and the over-pressure Δp. This relation is a Bernoulli equation for which we assume an incompressible, irrotational (because of the free jet formation) and quasi-stationary airflow. Assuming the volumic kinetic energy at the upstream of the reed to be considerably smaller than the downstream one in the free jet, when blowing, the Bernoulli equation between upstream and downstream of the reed is then:

$$\Delta p = \frac{1}{2}\rho_0 v_j^2 \tag{7}$$

where the effect of the viscosity is implicitly taken into account in the free jet formation assumption.

To complete the description of the flow through the reed, we now introduce the definition of the useful section.

2.3 Useful section

In this section, we review the different kinds of models for the useful section used in the literature and propose a new one which permits better temporal simulations.

2.3.1 Existing models for the useful section

The first model one may find for the useful section [37, 2, 38, 21, 12, 39, 40, 25, 41, 14, 34] considers that the flow issues from the instruments only by the front section of the reed (see Figure 2) and, in this case, its generic expression is then:

$$S_u = W_r.h_{up} \tag{8}$$

where W_r is the width of the reed at its tips and h_{up} the reed opening at the free-end for the upstream section. As this model does not consider the sides contribution, Cuesta and Valette [26] replace the width W by the global perimeter $2.L_r + W_r$ in equation (8). To take into account the fact that, during its motion, the free reed can go inside the thickness of its support or can even protrude through the other face of its support, Millot [34] assumes that the useful section is zero when the reed is inside the thickness of its support and that, in the other cases, the useful section is given by the product of the absolute value of the tip opening and the global perimeter. Indeed, it is necessary to consider the absolute value of the tip opening and not the algebraic tip opening because it will give negative values for S_u each time the reed goes inside the thickness of the support. But the assumption of a closure of the channel, when the reed is inside the thickness of its support, should be rejected because there is always at least a minimal opening due to the clearance gaps between the reed and its support (and, as illustrated by Figure 2, the front section is a not a rectangle of width W_r because of these clearance gaps). But, all these models consider the opening all over the reed constant, which is in contradiction with the nature of the free reed as illustrated on Figure 1.

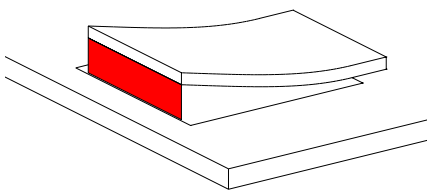

Figure 2: Illustration of the considered escape area in the case of the clarinet-like hypothesis: only a part of the front section is taken into account. This model is still used for the study of clarinet and saxophone, which use beating reeds, where it seems difficult to express the local deformations of the reed as a function of the displacement of the tip of the reed.

In the case of the model proposed by Tarnopolsky *et al* [28] and used by Hikichi *et al* [42], the useful section is calculated using the following expression:

$$S_u(h_n) = W_r\sqrt{h_n^2 + h_{min}^2} + 2.L_r\sqrt{a^2(h_n) + h_{min}^2}$$

where h_{min} is the gap width existing between the reed and its support when the reed is horizontal and $a(h_n)$ is the mean aperture under the reed which is calculated as a function of the tip opening h_n :

$$a(h_n) = h_{000} + \frac{1}{L_r}(h_n - h_{n,00}) \int_0^{L_r} \psi(s)ds$$

where h_{000} is the thickness of an optional lay, L_r is the length of the reed, h_n and $h_{n,00}$ are respectively the current and the rest openings at the tip of the reed, $\psi(s)$ the reed factor. If Hikichi uses this expression wherever the reed is (inside or outside the instrument) with an absolute value for $a(h_n)$, Tarnopolsky *et al* say that this expression is only valid if the reed does not enter the aperture block but do not give an expression for this case.

At almost the same time, Debut and Millot [43, 44] introduced a quasi similar model for S_u considering the case of a reed inside its support and also protruding through the other face of the support. But, in this model, the useful section is calculated all over the reed sides using a local effective opening noted $h_{eff}(s)$ rather than the mean aperture. The useful section is then given by:

$$S_u(h_n) = W_r\sqrt{h_n^2 + h_{min}^2} + 2.\int_0^{L_r} \sqrt{h_{eff}^2(s) + h_{min}^2}ds$$

with

$$h_{eff} = \begin{cases} h_n - e_r & \text{if} \quad h_n > e_r \\ 0 & \text{if} \quad h_n \in [-e_s, e_r] \\ -(h_n + e_s) & \text{if} \quad h_n < -es \end{cases}$$

where e_s is the thickness of the support, e_r is the thickness of the reed.

But, as illustrated by Figure 3, there are still some parts of the section under the reed which are not included in the calculation in these two models: a part of the lateral area and two triangles for the front section. The model proposed by Tarnopolsky *et al*, using a mean opening $a(h_n)$, assumes that all the lateral escape areas are oriented in the same direction which is false: the orientation of the normal to the local escape area changes all over the sides, from vertical at the clamped end to almost horizontal at the free end of the reed. This problem is almost solved by the model proposed by Debut and Millot with the use of an integral over the sides of the local openings under the reed.

In the model of Debut and Millot, there is still a problem with the definition of the useful section because, even if we do not have a zero S_u when the reed is inside its support, we change the frontiers of S_u when the reed is at the other side of the support. Indeed, with the definition of h_{eff}, we consider the effective height between the downstream face of the support and the downstream face of the reed, when the reed protrudes at the downstream face of the support, while we consider the upstream face of the support and the downstream face of the reed when the reed is inside the instrument. As this change is not natural we propose a new model for the useful section.

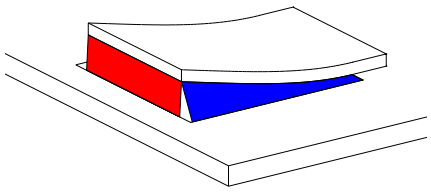

Figure 3: Illustration of the considered escape area in the case of the models used for the study of free reeds [28], of the sho [42] and for the study of chromatic playing on a diatonic harmonica [43, 44]. In these models, the flow is assumed to pass by the front of the reed and also by the sides of the reed. But one can see that the considered front and lateral areas are not complete and that the orientation of the local opening changes all over the length of the reeds.

2.3.2 New model for the useful section

We have seen that the existing models do not take account of the total section under the reed, as illustrated in Figure 3. We also have seen that there is some confusion between the neutral, upstream and downstream sections of the reed in the case of the definition of the useful section. We now propose another model which may solve this problems.

We need to distinguish (-,+) and (+,-) reed because the frontiers of the escape area are different and the expressions of the contributions of useful section change. For a (-,+) reed, we consider the escape area between the downstream face of the reed and the upstream face of the support while, for a (+,-) reed, the escape area is chosen between the upstream face of the reed and the downstream face of the reed. But, in both cases, we distinguish three contributions to the useful section: the front section; both sides sections limited by the free end of the reed as proposed by Tarnopolsky or Debut; the missing sides areas.

The first contribution is the front area, a trapezoid, as the floor frontier in the plane of the support includes the two clearance gaps between the reed and the window in the support (see figure 3). The expression for the front contribution is then:

$$S_{end} = (W_r + h_{min}).h_{end}$$

where h_{end} is the height of the trapezoid.

We can calculate the height of the trapezoid as the hypotenuse of a triangle whose sides are respectively the effective opening h_{eff} under the reed (illustrated by Figure 4 for both kinds of reed) and the length x_{eff} of the horizontal segment limited by the projection of the free-end point of the reed we consider and the end of the aperture in the support. The effective opening under the reed is given, in the (-,+) reed case by:

$$h_{eff} = |h_{do} + e_s|$$

and, in the (+,-) reed case by:

$$h_{eff} = |h_{up}|$$

We must emphasise that we find e_s in the expression of h_{eff} (an after in the expression of $h_{eff}(s)$) in the case of the (-,+) reed, just because we have chosen the same convention and origin for both reeds. In fact, e_s does not play a role in the whole determination of the useful section because it is also present, with a minus sign, in h_{do} and $h_{do}(s)$. If we had chosen as zero (deflection) point the upwards face of the reed, we would not have e_s in the expressions of S_u and we would be able to point out the fact that the expressions for S_u for a (-,+) reed are derived by replacing h_{do} by h_{up} in the expressions of S_u for the (+,-) reed: this change is also equivalent to replacing e_r by $-e_r$ when passing from the (+,-) case to the (-,+) case. So, there is no need to study the influence of the e_s parameter on the behaviour of the reed with the proposed model.

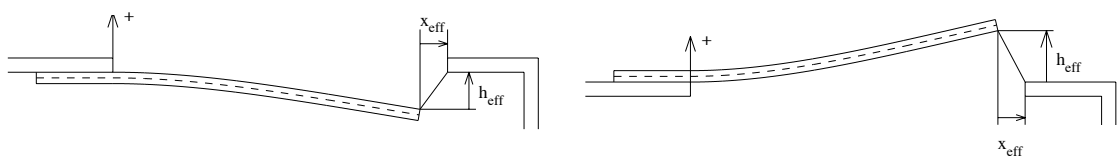

Figure 4: The height h_{end} of the trapezoid is illustrated by the segment linking the end point of the reed and the end point of the aperture in the support. One can also see the definition of both lengths h_{eff} and x_{eff} useful to calculate h_{end}. h_{eff} is the opening under the reed limited by the plane of the support. x_{eff} is defined as the length of the segment between the projection of the end point of the reed in the plane of the support and the end point of the aperture. These definitions are illustrated for both (-,+) reed (left) and (+,-) reed (right).

The end of the aperture in the support is situated at a distance $L_r + h_{min}$ from the clamped end and we consider that the projection of the end point of the reed is situated at a distance $L_r + \Delta x$ from the clamped end of the reed which gives for $x_{eff} = h_{min} - \Delta x$. For a (-,+) reed, as we need to consider the projection of the end point of the downstream face of the reed, Δx is then given by $\Delta x = \Delta x_{do}$ (see Appendix for details concerning the expressions of Δx_{do} and Δx_{up}). For a (+,-) reed, we consider the projection of the upstream face of the reed which gives a $\Delta x = \Delta x_{up}$. In these conditions, the height of the trapezoid is then:

$$h_{end} = \sqrt{h_{eff}^2 + (h_{min} - \Delta x)^2}$$

so that the front section is then given by:

$$S_{end} = (W_r + h_{min}).\sqrt{h_{eff}^2 + (h_{min} - \Delta x)^2}$$

The second contribution to the useful section is the one associated with the side escape areas delimited by the end of the reed as illustrated by Figure 5. To calculate the contribution of each portion of the reed we need to extend the definition of the effective height h_{eff} to $h_{eff}(s)$: $h_{eff}(s) = |h_{do}(s) + e_s|$ for a (-,+) reed and $h_{eff}(s) = |h_{up}(s)|$ for a (+,-) reed. We also need, for each portion of the reed, to consider the gap between the reed and its support to calculate the local effective opening under the reed and, for each side, integrate it over the length of the reed to find the side area:

$$S_{sides} = 2\int_0^{L_r} \sqrt{h_{eff}^2(s) + h_{min}^2}ds$$

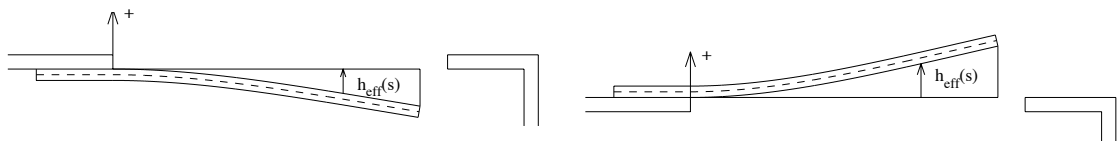

Figure 5: Illustration of the section under the reed and of the definition of the local effective height $h_{eff}(s)$ under the reed for (-,+) reed (left) and (+,-) reed (right). These side areas are limited by the face of the support involved in the calculation, by the associated face of the reed and by a vertical segment linking the plane of the support and the end point of the reed.

There are still two missing areas to complete the useful section: the areas of the triangles delimited by the end point of the reed, its projection in the plane of the support and the end of the aperture in the support. With the help of Figure 4, one can see that the side lengths of the triangles are respectively h_{eff} and x_{eff} so that the missing area is then derived as:

$$S_{tri} = h_{eff}.(h_{min} - \Delta x)$$

As shown on Figure 6, the area of the triangle needs to be algebraic because for some high magnitude openings of the reed, the end point of the reed is further than the end of the aperture in the support. This possibility is taken into account in the former expression of S_{tri} because $h_{min} - \Delta x$ can be positive or negative according to the position of the useful end point of the reed.

Finally we can write the expression of the useful section S_u, given by the sum of these three contributions, $S_u = S_{end} + S_{sides} + S_{tri}$, as :

$$S_u = (W_r + h_{min}).\sqrt{h_{eff}^2 + (h_{min} - \Delta x)^2} + h_{eff}.(h_{min} - \Delta x) + 2\int_0^{L_r} \sqrt{h_{eff}^2(s) + h_{min}^2}ds \quad (9)$$

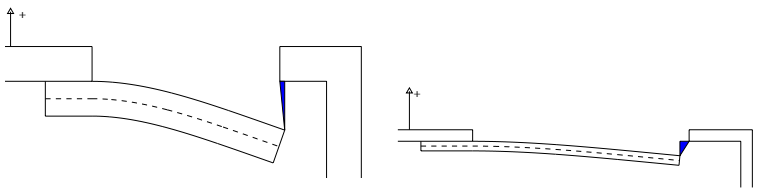

Figure 6: According to the opening of the reed, the triangle area needs to be negative (left) or positive (right) to compensate the defaults of the description of the sides sections under the reed. Indeed, the rotation of the cross section of the reed, for high magnitude openings and thick reed, can drive the end point further than the limit of the aperture in the support. In such cases, the area under the reed is bigger than the real area and needs to be corrected. This is the reason why S_{tri} is an algebraic area.

One must note that in certain circumstances there is a problem of intersection between the front area we have defined and the corner of the reed, as illustrated by Figure 7. To cope with this problem, it may be necessary to modify the definition of the frontiers. But, as we have a corner with sharp edges we can think there may be some flow separation and vortex shedding near the corner but we do not know how it will occur [45]. If we want to take account of these phenomena we may also have to consider the real 3D configuration for the flow through the reed, varying jet velocity along the reed and also variable overpressure all over the reed. But flow visualisations performed by Fabre [46] clearly indicate that we have some free jets all around the reed which may be a positive argument for our assumptions. Moreover, the pictures of the flows show that the orientation of the free jet depends on the opening of the reed: from a jet normal to the support when the reed is flat, we can see a rotation of the jet down to the support as the reed opening increases for the reed sides views and the reed front views. The rotation of the free jet for the sides or the front of the reed are explicitly taken into account in our model so we think it may correspond to a fair first approach: one can consider that we unfold both lateral section to consider only a so-called extended front section. As we want to keep a model as simple as possible we do not modify the model for the useful section to adopt a real 3D configuration.

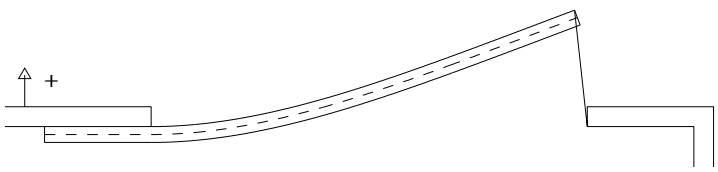

Figure 7: Illustration of a default of the proposed model. For some reed openings, the front area and the reed end intersect so the frontier may be different.

With the equations (4) to (7) and the definition of the useful section, the local description of the reed is not complete as there are still some missing data: the excitation

upstream of the reed and the "load" downstream of the reed. These additional assumptions permit definition of the different reed instruments and identification of easy playing conditions. A minimal configuration is proposed in the following to be able to study both (-,+) and (+,-) reeds.

3 Discussion of the minimal model

In this section, we illustrate the interest of the modification introduced for the useful section S_u for both (-,+) and (+,-) reeds and examine the assumptions used to derive the whole model. Some first results concerning the nature of the bifurcation for both reed are also given. We also study the infuence of the volume length L_1, of the excitation velocity v_0 and of the reed thickness e_r.

3.1 Minimal configuration

To be able to study both (-,+) and (+,-) reeds with the same conditions we introduce the configuration of Figure 8. In this configuration, we first encounter a volume V_1 in which the pressure p_1 is assumed to be uniform. This volume is supplied by a fixed volume flow u_0 and we adopt the adiabatic hypothesis for the volume: we use in fact the low Mach number approximation for the adiabatic hypothesis to derive the mass conservation equation. After the volume, we find a pipe of length L_2 and cross section S_2. In this pipe, we consider an irrotational and incompressible airflow (p_2 is uniform in the entire pipe) and also assume that the kinetic energies are much less important than the unsteadiness. We then find the reed, either a (-,+) or a (+,-) one, and, finally, the outside of the configuration where we assume to find the atmospheric pressure.

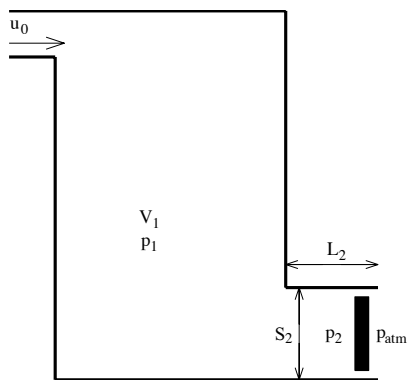

Figure 8: Configuration introduced to study both kinds of free reeds. The excitation is the constant volume flow u_0 supplying the volume V_1 where the pressure p_1 is assumed to be uniform. After the volume, one encounters a pipe of length L_2 and cross area S_2 upstream of the reed, in which the airflow is considered incompressible. Downstream of the reed the pressure is atmospheric.

In such conditions, the missing equations to get a complete reed problem are then:

- $\frac{V_1}{c_0^2}\frac{d(p_1 - p_{atm})}{dt} = \rho_0(u_0 - u)$, mass conservation for the volume V_1;
- $p_1 = p_2 + \rho_0 \frac{L_2}{S_2}\frac{du}{dt}$, Bernoulli equation for the pipe;
- $p_2 = p_{atm} + \frac{1}{2}\rho_0 v_j^2$, Bernoulli equation between the upstream and the downstream of the reed;
- $\frac{d^2\zeta}{dt^2} + Q^{-1}\omega_0\frac{d\zeta}{dt} + \omega_0^2\zeta = \mu(p_2 - p_{atm})$, reed motion equation;
- $u = S_r\frac{d\zeta}{dt} + \alpha S_u v_j$, total output volume flow equation.

To determine the conditions of reed instabilities, we calculate the expression of the upstream pressure p_2 as a function of ζ and its derivatives, using the Fourier transform of the linearized versions of the equations (see Appendix for details). The part of the over-pressure which is proportional to the derivative $\frac{d\zeta}{dt}$ may permit instability if its value is greater than $\frac{Q^{-1}\omega_0}{\mu}\frac{d\zeta}{dt}$.

Given the symmetry of the laws for the useful section (see Figure 9), we assume that $S_u = S_{u00} + a_1(h_n - h_{n,00})^2$ is a fair approximation of the useful section near the mean opening. In the following, to simplify the expressions we introduce $\zeta_0 = h_{n,0} - h_{n,00}$ where $h_{n,0}$ is the mean opening, $\zeta_{00} = h_{n,00} - h_{n,000}$, $S_{u0} = S_{u00} + a1(\zeta_0 - \zeta_{00})^2$. We also use the prime suffix for the variable or acoustical part of quantities used in the calculation: ζ' is for instance the acoustical part of ζ while ζ_0 is the mean value of ζ.

With linearization of the equations and some further calculation, the Fourier transform of p_2' can be written:

$$P_2'(\omega) = \frac{-\rho_0\big(1 - \frac{V_1 L_2}{c_0^2 S_2}\omega^2\big)}{\big(\frac{\alpha S_{u0}}{v_{j0}}\big)^2\big(1 - \frac{V_1 L_2}{c_0^2 S_2}\omega^2\big)^2 + \big(\frac{V_1}{c_0^2}\omega\big)^2}.\Bigg[\alpha A\frac{\alpha S_{u0}}{v_{j0}}\big(1 - \frac{V_1 L_2}{c_0^2 S_2}\omega^2\big) + \omega^2 S_r\frac{V_1}{c_0^2} + \mathrm{j}\omega\left(S_r\frac{\alpha S_{u0}}{v_{j0}}\big(1 - \frac{V_1 L_2}{c_0^2 S_2}\omega^2\big) - \alpha A\frac{V_1}{c_0^2}\right)\Bigg].\zeta'(\omega) \quad (10)$$

where $A = 2a_1(\zeta_0 - \zeta_{00})v_{j0}$.

description	notation	value
length of the reed	L_r	12.95 mm
width of the reed	W	2.1 mm
thickness of the reed	e_r	110 μm
thickness of the support	e_s	900 μm
rest departure from flat reed position	$\Delta h_{n,00}$	528 μm
rest reed opening	$h_{n,00}$	
	(-,+) reed	$-\Delta h_{n,00} - \frac{e_r}{2} - e_s$
	(+,-) reed	$\Delta h_{n,00} + \frac{e_r}{2}$
clearance gaps width	h_{min}	50 μm
eigen frequency	f_r	444 Hz
equivalent reed stiffness	K	47.9 N.m^{-1}
quality factor	Q	95

Table 2: Mechanical and geometrical characteristics common for both tested reed. These characteristics were found for a (+,-) reed of a G diatonic harmonica on channel 4 (Lee Oscar^{TM} model) [35].

One can see that the condition for instability implies that:

$$\big(1 - \frac{V_1 L_2}{c_0^2 S_2}\omega^2\big)\big[S_r \frac{\alpha S_{u0}}{v_{j0}}\big(1 - \frac{V_1 L_2}{c_0^2 S}\omega^2\big) - \alpha A \frac{V_2}{c_0^2}\big] < 0$$

which may be verified for (-,+) and (+,-) reeds because we can play, at least, on the signs of two factors: $1 - \frac{V_1 L_2}{c_0^2 S_2}\omega^2$, depending of the volume and pipe dimensions and A depending of the nature of the reed. In fact, as $A > 0$ for a (+,-) reed we must have $1 - \frac{V_1 L_2}{c_0^2 S_2}\omega^2 > 0$ while, as $A < 0$ for a (-,+) reed, we must have $1 - \frac{V_1 L_2}{c_0^2 S_2}\omega^2 < 0$.

The keypoints for the numerical simulations are given in the Appendix.

As the proposed configuration may permit the instabilities of both kinds of reed, we can now give some numerical results with this minimal model.

3.2 Illustration of the minimal model

In this subsection we apply the model for two reeds, with the same geometrical and mechanical properties but with a different settlement: one (-,+) reed and a (+,-) another one. The geometrical and mechanical properties are given by Table 2.

For this comparison, we compute, in time domain, the system of equations for the minimal model. We assume constant the parameters given by Table 3 but we consider variable values for the feeding velocity v_0 ($u_0 = S_0.v_0$), the length of the volume 1 according to the considered reed.

description	notation	value
cross section area of the feeding pipe	S_0	30 mm^2
cross section area of the volume 1	S_1	800 mm^2
length of the pipe 2	L_2	20 mm
cross section area of the pipe 2	S_2	25 mm^2

Table 3: Constant geometrical dimensions for the configuration used to study both (-,+) and (+,-) reeds.

The laws of the useful section for both reeds are given in Figure 9. One can see that, as the differences between the reeds is only the settlement, we have the same laws but translated: for the (-,+) reed the law is centered around $h_n = -e_s - \frac{e_r}{2}$ while, for the (+,-) reed, the center is at $h_n = \frac{e_r}{2}$. In fact, in both cases, we find that the centre corresponds to the flat reed position and that the law seems symmetrical which is normal because the neutral section is at the centre of the thickness which gives symmetrical displacements of points of both upstream and downstream sections around the points of the neutral section.

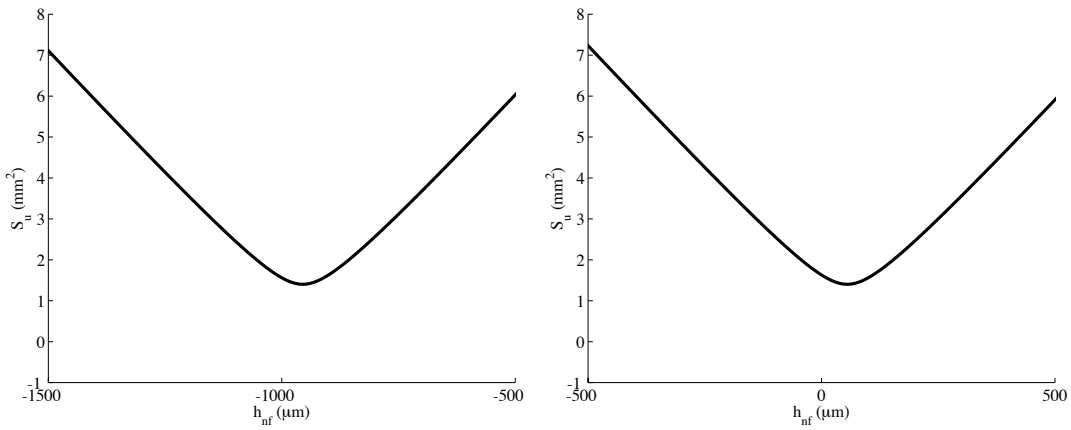

Figure 9: Illustration of the laws for the useful section S_u as a function of the neutral section displacement h_n in the case of a (-,+) reed (left) and in the case of a (+,-) reed (right).

Plots of figure 10 illustrate the behaviour of the three models of useful sections (Millot, Hikichi and Debut) for an excitation composed of the three steady portions separated by zero portions: we tried to be as close as possible to a triplet using steady excitations. These simulations are performed for both (-,+) and the (+,-) reeds and one can notice that while the three models seem to give quite similar simulations for a (+,-) reed, the results are rather different for a (-,+) reed. The Hikichi and Debut models give rather similar results compared to the Millot model which reacts more quickly.

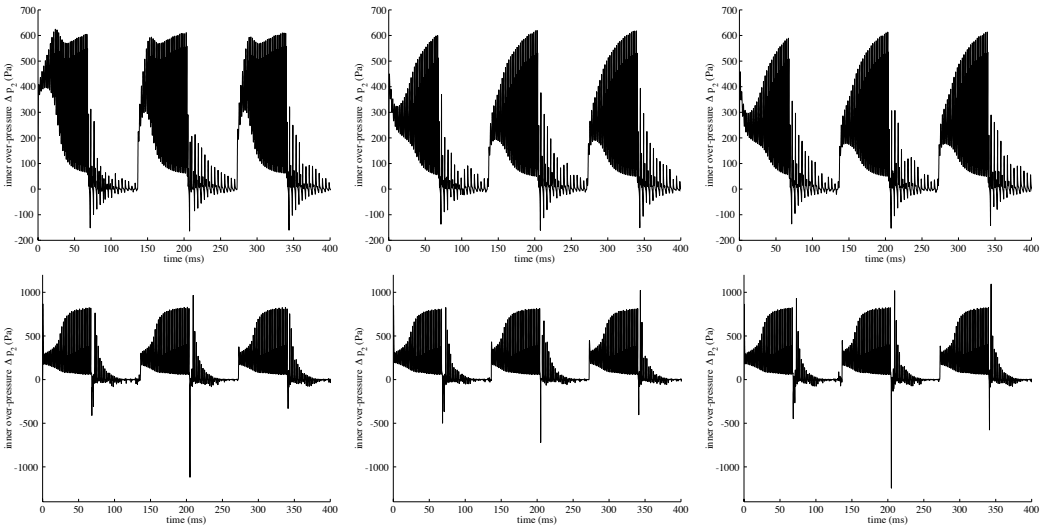

Figure 10: Illustration for blown notes of the different dynamical behaviours of a reed while using Millot (left), Hikichi (centre) or Debut (right) model for the useful sections. (top) waveforms for the (-,+) reed: $L_1 = 1.5$ cm, $v_0 = 3$ m.s^{-1}. (bottom) waveforms for the (+,-) reed: $L_1 = 8$ cm, $v_0 = 2.5$ m.s^{-1}. Numerical simulations are performed using three repetitions of 3000 samples with constant excitation signal v_0 followed by 3000 zeros in order to simulate an artificial but dynamic excitation close to a musical triplet.

Figure 11 present zooms on the attack phases for the three models and both reeds. For the (-,+) reed the difference of dynamic behaviour for the Millot model is quite obvious and shows that the reed answer is stronger and faster. For the (+,-) case, one can notice that there are some small temporal shifts in the answer of the reed and some tiny differences for the magnitude of the response. These small temporal shifts can also be seen with the plots of zooms on the steady part of the signals (see figure 12) for both reeds and the three useful section models. With these three figures, we can suggest that our new model present some significant differences at least for the transient part of the reed response in pressure.

To demonstrate this difference for the dynamic behaviour, we also present the numerical simulations performed using a more realistic excitation, the one presented in figure 13 and derived from the very lowpass filtering of a measured over-pressure signal inside a diatonic harmonica.

On figure 14, the whole signals for the over-pressure are only presented in the case of a (-,+) reed. Indeed, the differences are quite tiny in the (+,-) case as noticed for the artificial "triplet" excitation so we have chosen to concentrate on the (-,+) case. While the attacks are obviously different, the rest of the waveforms appear rather similar for the three models. It is also interesting to notice that the over-pressure envelope seems to follow the excitation curve in three cases after the transient phases. With the whole waveform plots, we can only note that the Millot model gives a more reactive reed while

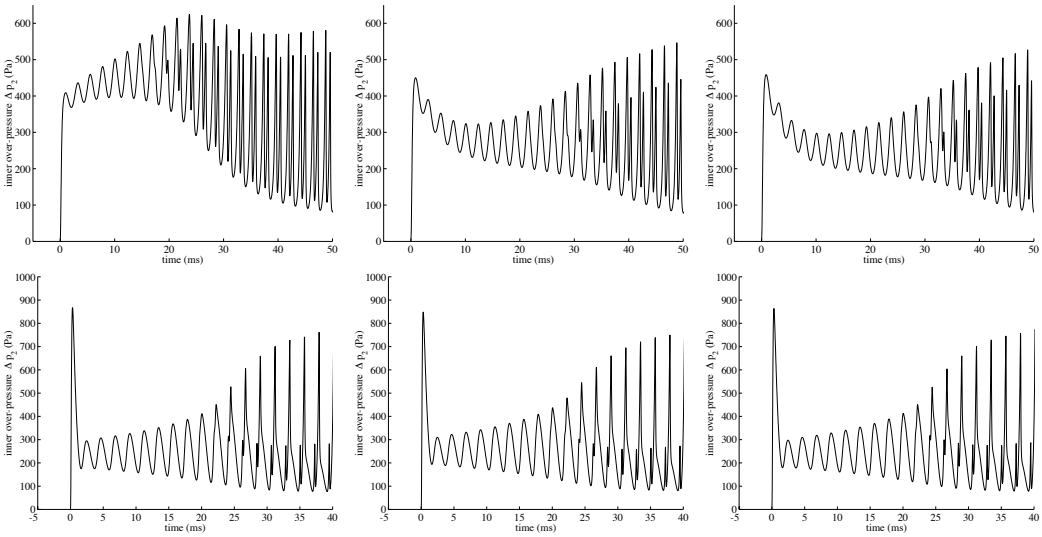

Figure 11: Zooms on the beginings of the plots of figure 10 which illustrate the different dynamical behaviours of a reed while using Millot (left), Hikichi (centre) or Debut (right) model for the useful sections. (top) waveforms for the (-,+) reed ; (bottom) waveforms for the (+,-) reed.

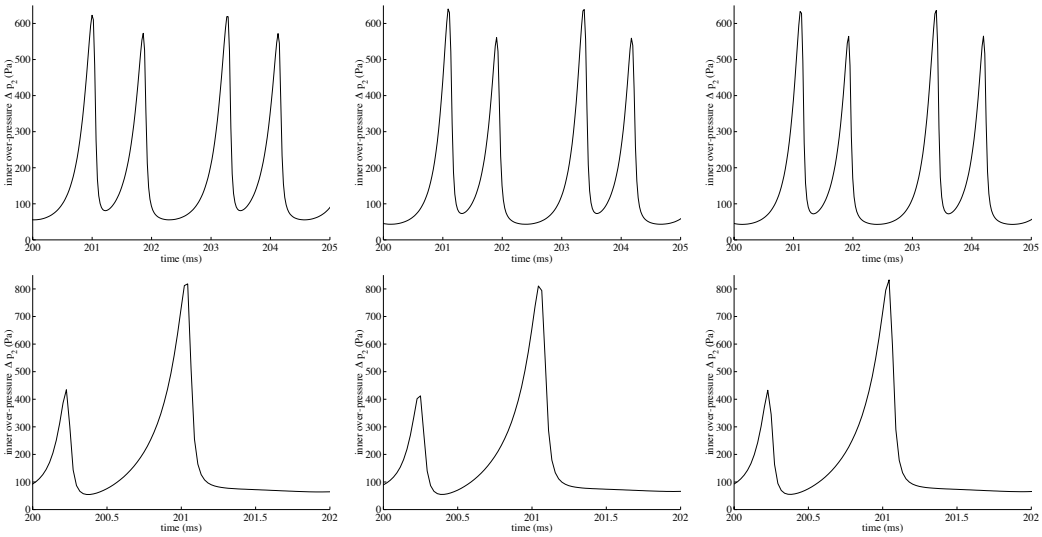

Figure 12: Zooms on the steady parts of the plots of figure 10 which illustrate the different dynamical behaviours of a reed while using Millot (left), Hikichi (centre) or Debut (right) model for the useful sections. (top) waveforms for the (-,+) reed ; (bottom) waveforms for the (+,-) reed.

the Hikichi model gives a later departure.

With figure 15, the attention is focused on the transients which really point out the great differences of the dynamical behaviour of the reed according to the useful section

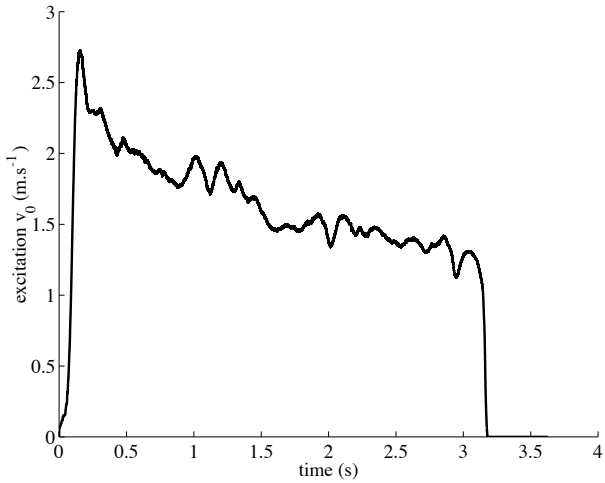

Figure 13: Plot of the dynamic excitation used for the following numerical simulations.

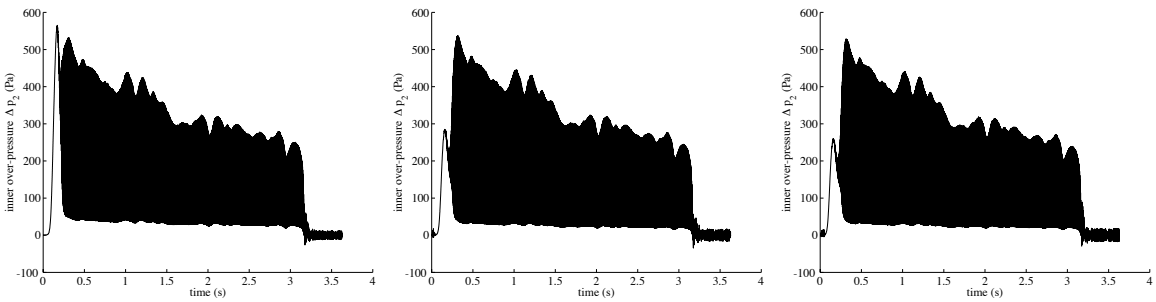

Figure 14: Another illustration, using the dynamic excitation (see figure 13) of the different dynamical behaviours of a (-,+) reed while using Millot (left), Hikichi (centre) or Debut (right) model for the useful sections. The parameters are the following: $L_1 = 8$ cm, mean $v_0 = 1.35$ m.s^{-1}. One can notice that the reed does not have the same temporal response during the attack, according to the useful section model : fastest reaction is found for Millot model but the rest of the waveform seem quite similar.

model. The Millot model reacts earlier and more strongly than the two other which may correspond to a more reactive reed configuration. The Debut model follows, and the third reed to react is the one using the Hikichi model. These differences for the reed transients constitute a strong argument to search a useful section as precisely as possible even in the case of a simplified model. So, even if our model presents a more complex formulation we do think it must be carefully considered. Moreover, to perform numerical simulations, it is always possible to calculate tables for the useful sections before beginning the temporal simulations which permits access to shorter times for the calculation.

3.3 Discussion of the assumptions

In this section, we review the assumptions we have made to derive the proposed model and discuss their validity.

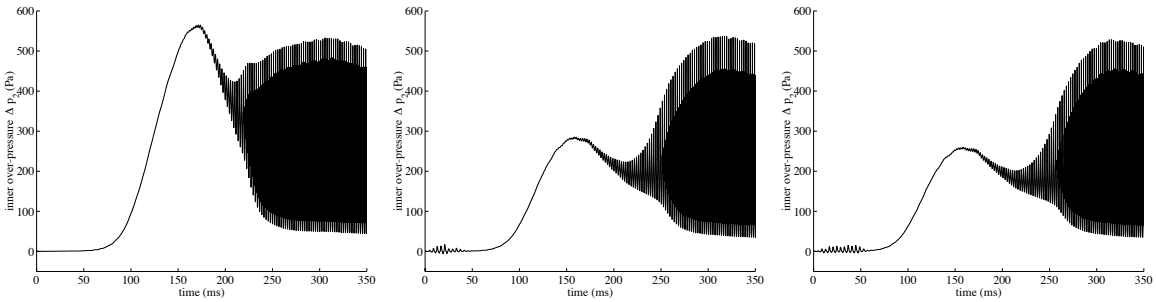

Figure 15: Zooms on the beginnings of the plots of figure 13 which illustrate the different dynamical behaviours of a reed while using Millot (left), Hikichi (centre) or Debut (right) model for the useful sections. One can notice that the Millot model gives a fast and more reactive reed with a rather different behaviour, Hikichi model gives a reed which reacts the most slowly.

For all the results presented in this section, the parameters for the (-,+) reed were $L_1 = 8$ cm and $v_0 = 2.5$ m.s^{-1} while for the (+,-) reed we used $L_1 = 1.5$ cm and $v_0 = 3$ m.s^{-1}.

Figures 16 respectively illustrate the waveform and the power spectrum for the upstream/downstream over-pressure $\Delta p_2 = p_2 - p_{atm}$ in the case of a (-,+) or a (+,-) reed. We can not compare these results with experimental results because we adopt the reed properties for the (+,-) reed of the fourth channel of a diatonic harmonica while both (+,-) and (-,+) reeds have different properties on a diatonic harmonica. Moreover, we do not have the experimental setup associated with the loading configuration we propose. Yet the waveforms and the spectrums found for both (-,+) and (+,-) are realistic compared to real blows and overblows produced on a diatonic harmonica. And, when one uses a time-varying excitation, the sound produced is quite realistic for the listener. But an experimental validation should be done for the one reed case; an experimental validation for a two reeds case will be presented elsewhere, in the case of chromatic playing on diatonic harmonica.

With the Figure 17, the sinusoidal nature of the neutral section displacement is confirmed as proposed in [35] for harmonica reeds with a playing frequency under the reed eigen reed frequency f_r in the case of the (-,+) reed and over f_r in the case of the (+,-) reed as it is shown in the following. In both cases, the reed displacement is important and the reed goes inside the thickness of the support during a noticeable part of the period. The thickness of the reed is illustrated by both dashed lines around the solid line, associated with the flat position for the reed. This thickness does not seem so tiny compared to the whole magnitude of the reed displacement or to the support thickness so we think we should not neglect it in the reed model.

The space between the zero line and the first other dashed line corresponds to the inside of the support so both reeds vibrate inside the thickness of the support and, for very long

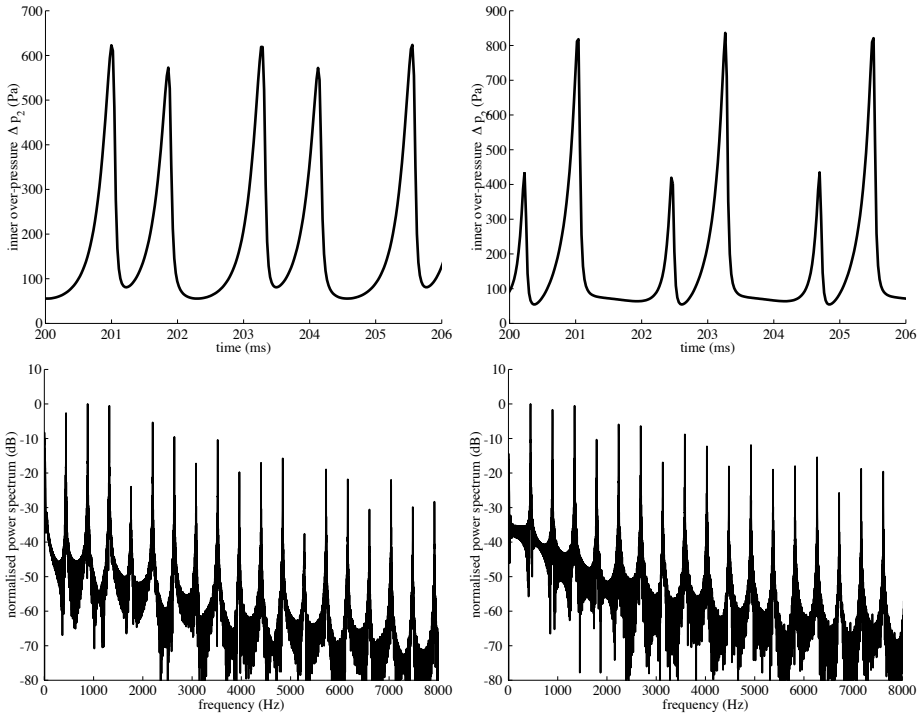

Figure 16: (top) Waveforms for the over-pressure Δp_2 for the (-,+) reed (left) and the (+,-) reed (right). (bottom) Related normalised spectra.

reeds (low frequency ones on a diatonic harmonica) the reeds can even go through the whole thickness of the support.

One can note that the signal is calculated with a little length L_1 (1.5 cm) in the case of the (+,-) reed while we have a long length L_1 (8 cm) in the case of the (-,+) reed. This is in accordance with the instability conditions we have found in the precedent subsection: little L_1 makes easier the verification of the instability condition in the case of a (+,-) reed while it makes harder the verification of the instability condition in the case of a (-,+) reed. This discussion is more developed in next subsection with the study of the influence of the variation of L_1 for both reeds.

In the model, we propose to take account of the flow displaced by the reed, the pumped flow. This assumption is justified because the pumped flow represents a significant contribution to the output volume flow as illustrated in Figure 18 so this phenomenon must be taken into account in a minimal free reed model. It may be interesting to quantify the role played by the pumped flow in the radiated sound, because we have two contributions per reed: the pumped flow and the flow passing through the reed, whose natures are quite different. We suspect that the pumped flow contributes mainly to the low frequency part of the sound (because of its sinusoidal character) while the flow passing through the reed may mostly feed the high frequency part of the sound because it is related to the high non linearity of the flow through the reed (non linearity associated with the useful section

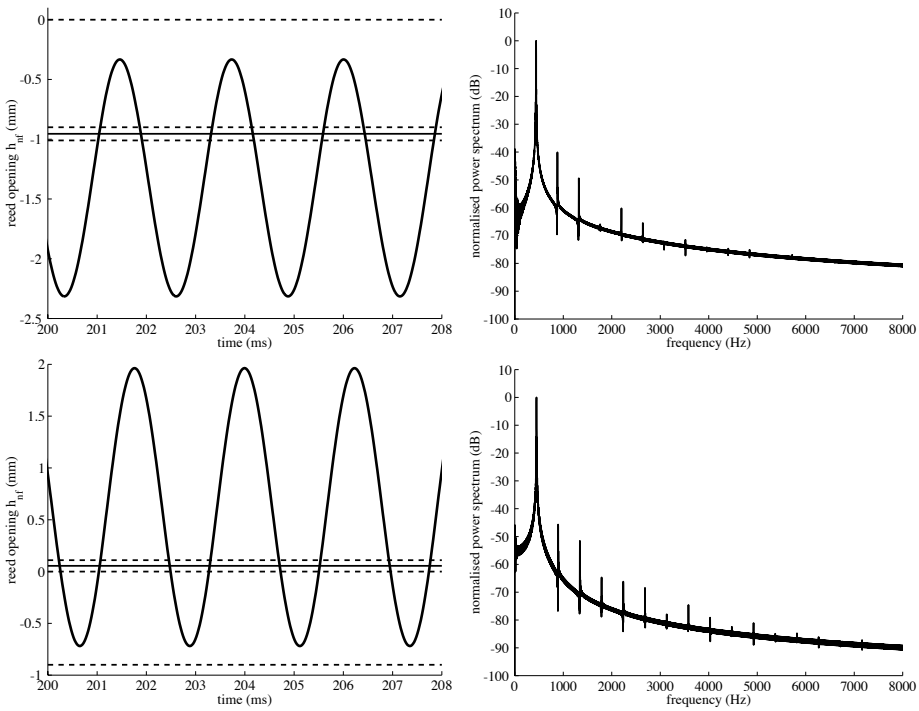

Figure 17: Waveforms for the neutral section opening and related normalised power spectrum in a case of a (-,+) reed (top) and of a (+,-) reed (bottom). For the waveforms, the solid plot indicates the flat position for the reed (no deformation case) while the dashed plots correspond respectively to the zero reference line, and the $\pm\frac{e_r}{2}$ departure from the flat position.

and the jet velocity).

With the Figure 19 we illustrate the behaviour of the over-pressure Δp_1 for the volume 1, the behaviour of the airflow velocity in the pipe and of the velocity in the free jet forming downstream of the reed. For the derivation of the Bernoulli equations for the pipe and through the reed we used the incompressible assumption. This assumption seems realistic considering the order of magnitude of the over-pressure Δp_2 (respectively 570 Pa and 783 Pa) and the fact that the Mach numbers are lower than 0.1: the compressibility of the air may be lower than 1 %. It seems also a fair first approach to consider the low Mach number approximation of the adiabatic relation to derive the mass conservation for volume V_1. We neglect the kinetic terms for the Bernoulli equation for the pipe 2 and this seems a valid assumption considering the differences of order of magnitude between the velocity v_2 and the over-pressure Δp_2: the contribution of the insteadiness is dominant in Δp_2 and neglecting the role of $\frac{1}{2}\rho_0 v_2^2$ seems reasonable as the Strouhal number $S_{t2} = \frac{L_2 . f_{play}}{v_{20}}$ is greater than one (respectively 2.93 and 2.49). For the Bernoulli equation between upstream and downstream of the reed, we also do not consider the upstream kinetic energy and this is a fair assumption when considering the respective

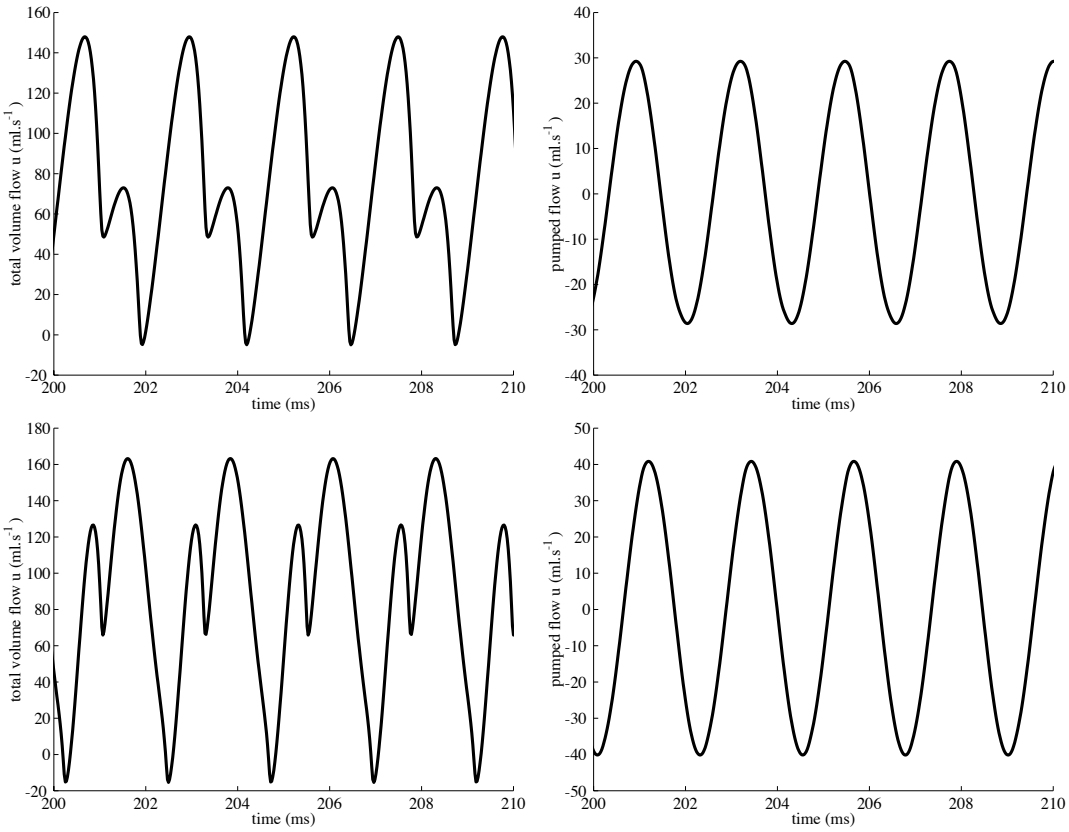

Figure 18: Waveforms for the total volume flow u (left) and for the pumped flow u_p (right) in a case of a (-,+) reed (top) and of a (+,-) reed (bottom). One can note that the pumped flow plays a significant role in the temporal evolutions of the total volume flow.

orders of magnitude for v_2 and v_j. We also consider the airflow quasi-stationary through the reed which seems realistic with a Strouhal number $S_{tr} = \dfrac{e_s.f_{play}}{v_{j0}}$ much lower than unity (respectively 0.024 and 0.027). The Reynolds numbers in the pipe and through the reed (considering the square root of the minimal useful section as equivalent diameter) are greater than 1235 which may mean that the viscosity effect are much lower than the other phenomena in the case of the free reed, which justifies that we do not consider explicitly the viscosity in this model.

3.4 Influence of the length L_1

In Figure 20, we study the influence of the pipe length L_1 over the playing frequency for both (-,+) and (+,-) reeds. We still used an excitation velocity of 2.5 m.s^{-1} for the (-,+) reed and of 3 m.s^{-1} for the (+,-) one and the other parameters were kept constant.

The playing frequency is almost independent of the volume V_1 in the case of the (-,+) reed (variation of 2.6 Hz) but it decreases when V_1 increases in the case of the (+,-) reed with a great variation of 22.2 Hz. It is also interesting to note that the playing frequency is

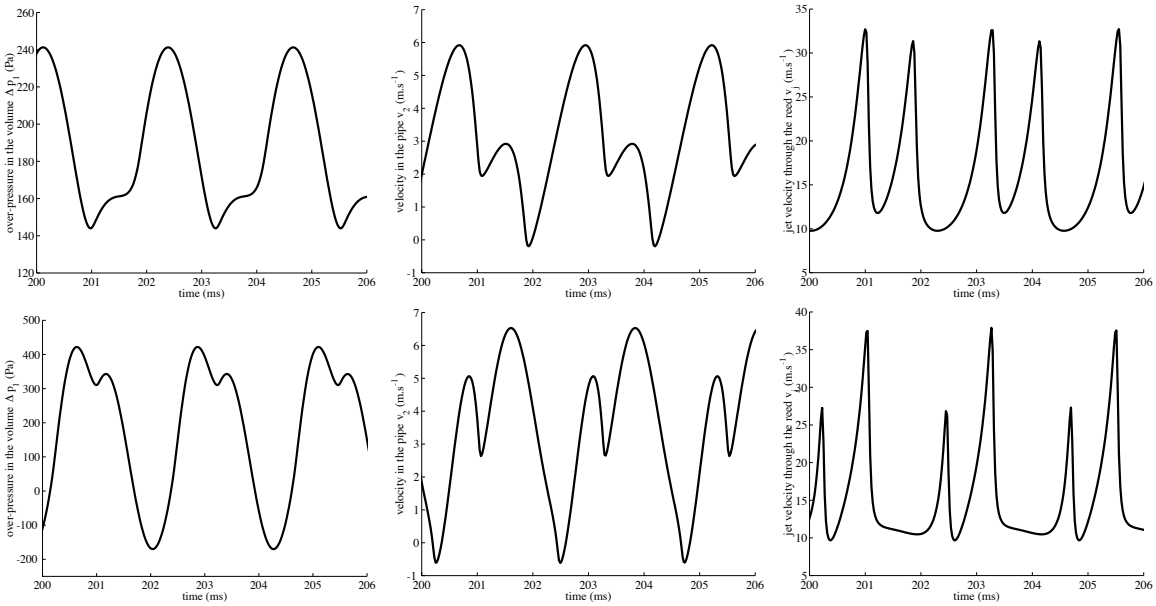

Figure 19: Waveforms for the neutral over-pressure Δp_1 (left) in the volume V_1, for the velocity v_2 in the pipe 2 (middle) and for the jet velocity v_j (right) in a case of a (-,+) reed (top) and of a (+,-) reed (bottom). One can note that the variations of the over-pressure are significant and that the velocities are important, above all in the free jet at the downstream of the reed which give high Reynolds numbers.

lower than the eigen frequency for the (-,+) reed and higher for the (+,-) reed as predicted by Helmholtz [1] and experimentally verified by Jonhston [24], Millot [34, 35] or Bahnson [16].

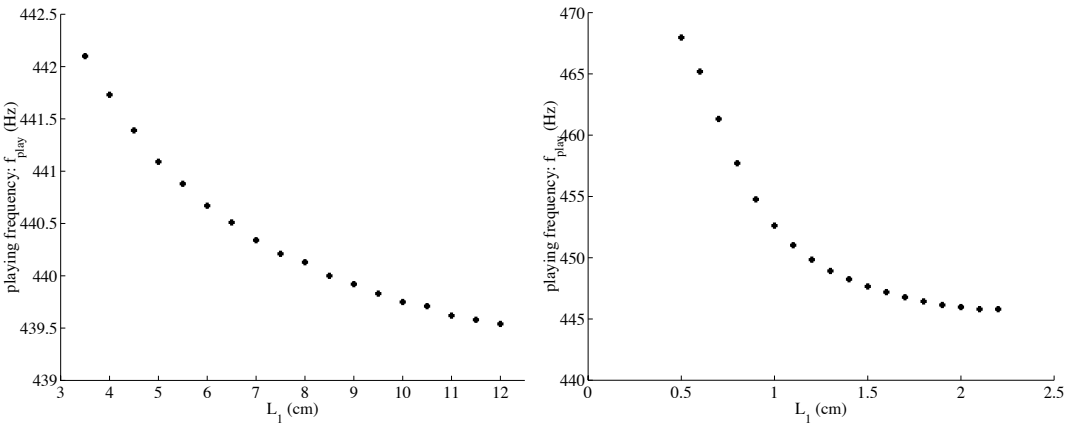

Figure 20: Influence of L_1 length on the playing frequency for a (-,+) reed (left) and a (+,-) reed (bottom) using respective excitation velocities v_0 of 2.5 and 3 m.s^{-1}. The playing frequency weakly varies for the (-,+) reed but presents great variations for a (+,-) reed.

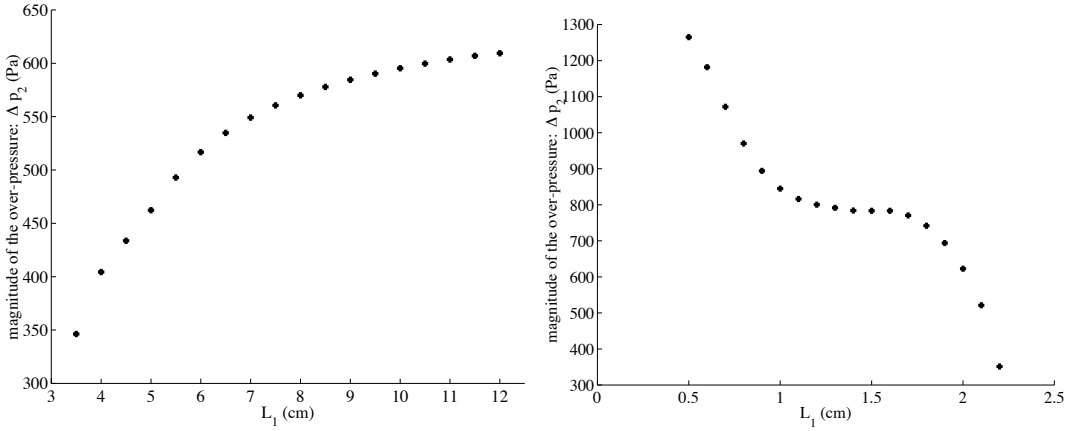

Figure 21: Influence of L_1 length over the magnitude of the over-pressure Δp_2 for (-,+) reed (left) and a (+,-) reed (right) using respective excitation velocities v_0 of 2.5 and 3 m.s^{-1}. Both reeds present great variations of the magnitude of Δp_2 but there is a flat-like part in case of the (+,-) reed.

On Figure 21, we have plotted the evolution of the magnitude of the over-pressure Δp_2 as a function of L_1. We can note that the influence is different for both reeds because the magnitude increases with L_1 for the (-,+) reed while it decreases for the (+,-) reed. This result seems coherent with the instability conditions derived for both reeds: having a little V_1 is a good thing for the instability of a (+,-) reed because we must have $1 - \frac{V_1 L_2}{c_0^2 S_2}\omega^2 > 0$ while, for a (-,+) reed, a little V_1 is a worse thing because we must have $1 - \frac{V_1 L_2}{c_0^2 S_2}\omega^2 < 0$. We can say that there are some convergence between the instability conditions and the results of the simulations.

We can also note that the variation of Δp_2 is greater in the case of the (+,-) reed (914 Pa) compared to the (-,+) reed (263 Pa) which may be related to the bigger variation of the playing frequency in the (+,-) case and with the fact that the (+,-) reed vibrates above its eigen frequency when blown.

3.5 Influence of the excitation velocity v_0

We also have studied the inluence of the excitation parameter v_0 for both reeds and the results for the playing frequency and the magnitude of Δp_2. Results for the playing frequency for both reeds are shown on Figure 22 while the ones for the magnitude of Δp_2 are given on Figure 23.

For each reeds, we started from rest and first searched the v_0 for which the reed produces sound. Then, we increased the excitation velocity up to 10 m.s^{-1} and plotted all these points with crosses. After, we decreased the excitation velocity v_0 until the velocity for

which it was impossible to maintain sound production and plotted all these plots with boxes.

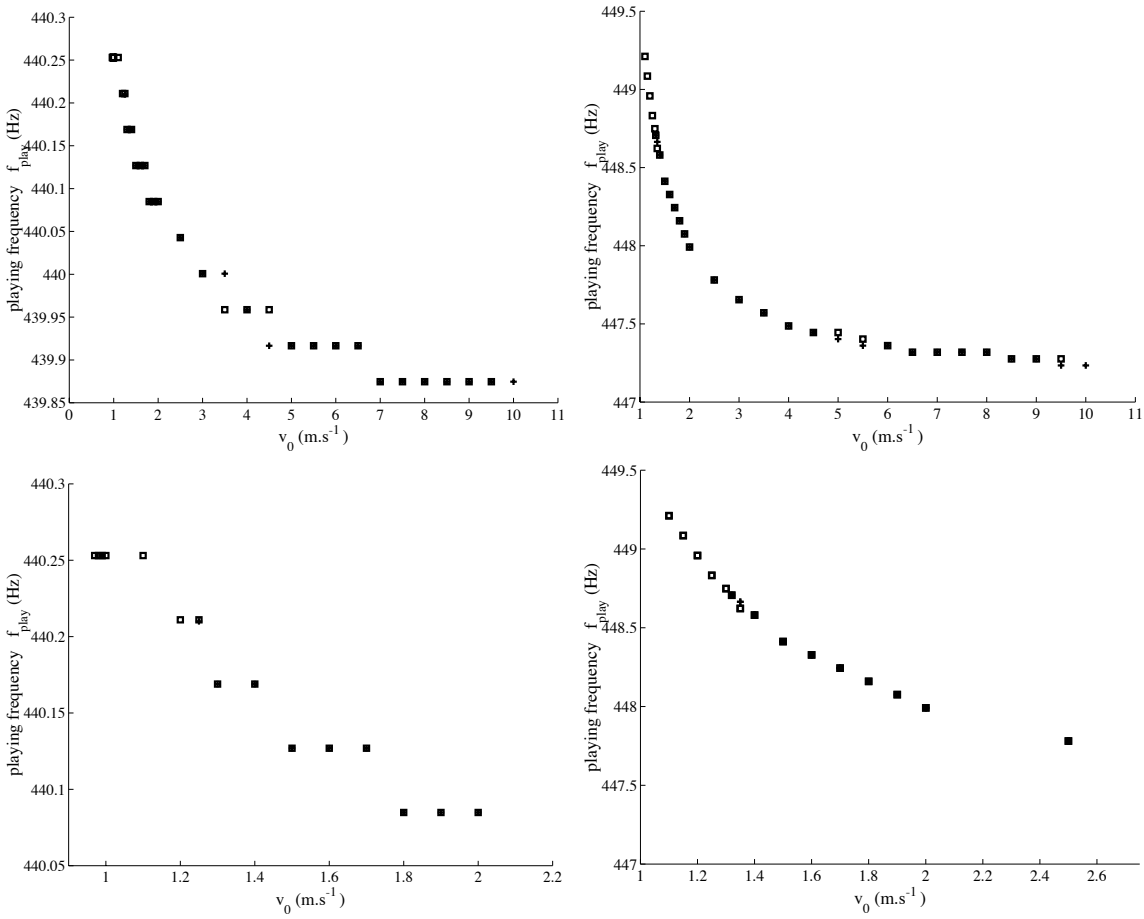

Figure 22: Plots of the variation of the playing frequency when the velocity excitation v_0 varies for a (-,+) reed (left plots) and a (+,-) reed (right plots). Top curves illustrate the case for the whole range of excitation while bottom curves present a zoom on the first values of v_0. We use crosses when v_0 increases and boxes when v_0 decreases.

The variation of the playing frequency is quite weak when the excitation velocity varies whatever is the type of the reed: 0.4 Hz for the (-,+) reed and 2 Hz for the (+,-) reed. But, we can note that, for both reeds, we can decrease the excitation velocity and still produce sound once the sound production mechanism is launched.

One can notice that we have a similar phenomenon for the magnitude of the overpressure Δp_2 but with great variations according to excitation velocity: 2780 Pa for the (-,+) reed and 3177 Pa for the (+,-) one. We still observe that we can decrease the excitation once the sound production is established for both reeds. And we observed, probably, the same kind of phenomenon during the recordings with a real musician on a diatonic harmonica for all kinds of note (normal blown and drawn notes, blown and

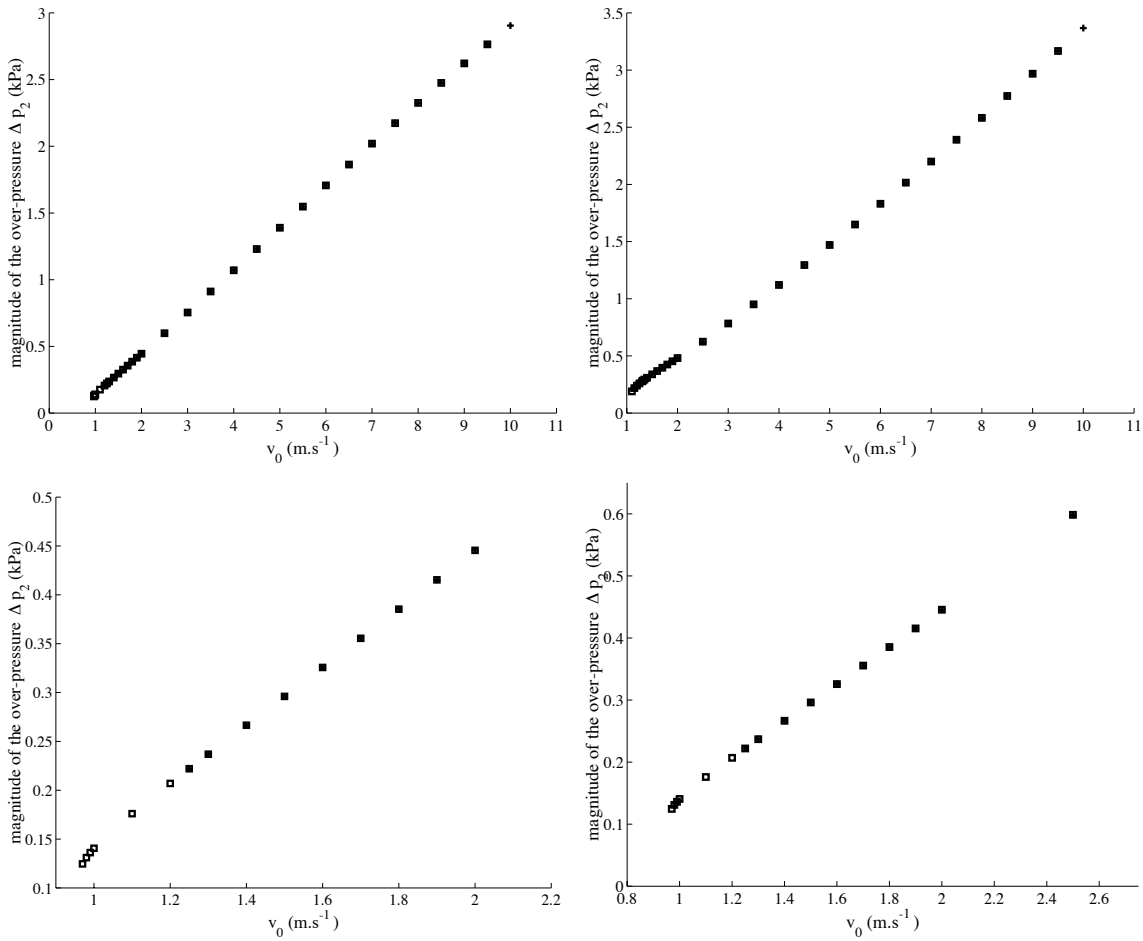

Figure 23: Plots of the variation of the magnitude of the over-pressure Δp_2 when the velocity excitation v_0 varies for a (-,+) reed (left plots) and a (+,-) reed (right plots). Top curves illustrate the whole range of excitation while bottom curves present a zoom on the first values of v_0. We use crosses when v_0 increases and boxes when v_0 decreases.

drawn bends, overblows and overdraws). For each recorded note, we had a waveform quite similar to the one given in Figure 24.

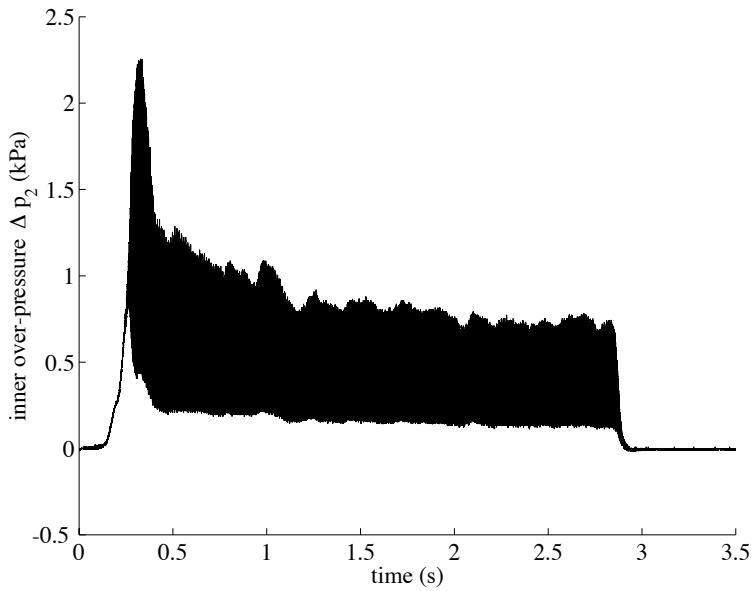

Figure 24: Example of a waveform for the over-pressure Δp_2 measured on a diatonic harmonica as played by a musician. This waveform shows a strong attack level for the over-pressure and then a lower "sustain" part of the signal. We found such configuration for all the sounds produced by the musician which may indicate that it is important to take a violent attack to get the production of the sound.

In Mechanics, there are the notions of direct and inverse bifurcations. A direct bifurcation corresponds to the situation where the oscillation is obtained from a threshold value of the excitation but with a magnitude of the response growing continuously from zero to the maximal possible value. And, for a direct bifurcation, while decreasing of the excitation we follow exactly the same curve up to the threshold point. For an inverse bifurcation, it is impossible to observe a continuous departure from a zero magnitude response: there is a step in the response. And, moreover, it is possible to maintain the response for lower excitation levels once the response is established: one can decrease the excitation once the sound is established (for a musical instrument for instance) and still observe sound production for a little range of excitations lower than the threshold one.

From the study of the influence of the excitation parameter, we can see that both reeds seem to present an inverse bifurcation because the sound production begins with a violent step in over-pressure and also because sound production can be maintained while decreasing the excitation level over a small range.

3.6 Influence of the reed thickness

To keep constant the reed mass while varying the thickness we must also change the value of either the reed length or the reed width. So, in the following, we study the influence of the variation of the thickness with, firstly, a related variation of the reed length L_r and, secondly, a related variation of the reed width W_r.

We do not study the influence of the variation of the support thickness e_s because this thickness is only present in the model to consider the same reference for both kinds of free reeds. Indeed, if we carefully consider the expression of the effective height, at the reed tip or for a local point on the reed side, we can verify that the support thickness has absolutely no effect on the useful section within the proposed model.

3.6.1 Case of varying reed length L_r

Figure 25 presents the evolution of the minimum, mean and maximum over-pressure Δp_2. These two plots show that the magnitude of the over-pressure decreases as the reed thickness increases, for both reeds. Indeed, the minimum over-pressure increases faster than the maximum over-pressure for both reeds. The average over-pressure also increases but still remains quite close to the minimum over-pressure which is related to the nature of the signals: fast succession of sharp peaks. This could be considered as a reason to think that the mean over-pressure has only a mathematical sense as the signal is seldom closed to its mean value. This is an argument to consider an acoustical flow rather than a mean flow with acoustical perturbations.

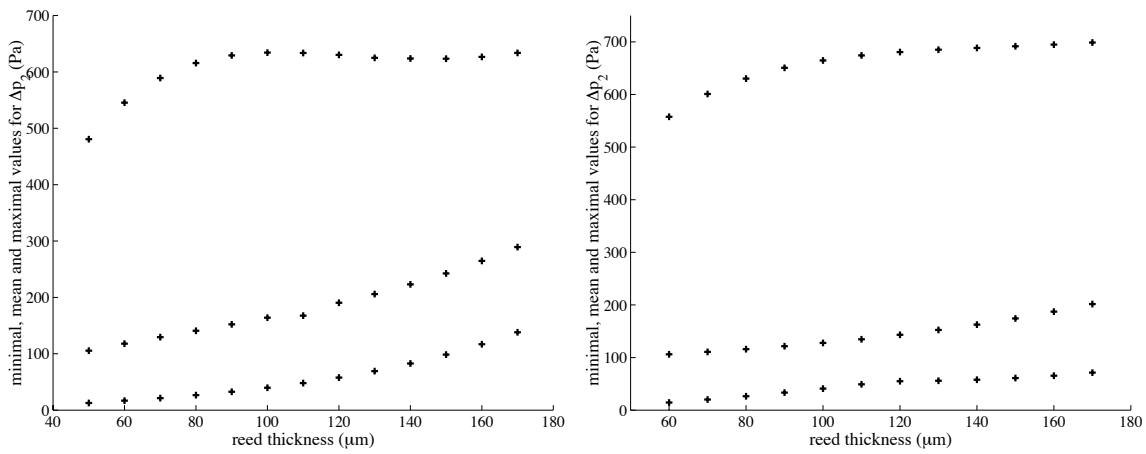

Figure 25: Influence of the variation of e_r, and L_r, over the over-pressure Δp_2 for a (-,+) reed (left) and a (+,-) reed. The values for the minimum, mean and maximum over-pressure are systematically plotted. The influence on both reed seems quite similar as all the values increase with the reed thickness. But the (+,-) reed present weaker reductions of the magnitude.

Influence of the reed thickness over the playing frequency is illustrated in Figure 26. One can see that the evolutions of the playing frequency are different according to the kind of reed we consider. Indeed, the playing frequency increases with the reed thickness for a (-,+) reed but still remains lower than the reed eigen frequency (444 Hz). For the (+,-) reed we have an inverse result as the playing frequency decreases when the reed thickness increases. But, even if the playing frequency decreases, it is still higher than the reed eigen frequency. It is also interesting to point out the fact that the variation of the playing frequency is a little larger for the (-,+) reed while we had the inverse result when we studied the influence of the volume V_1 or of the excitation velocity v_0 (even if in this case the variations were tiny). So varying the reed thickness have a strong influence over the note to be played.

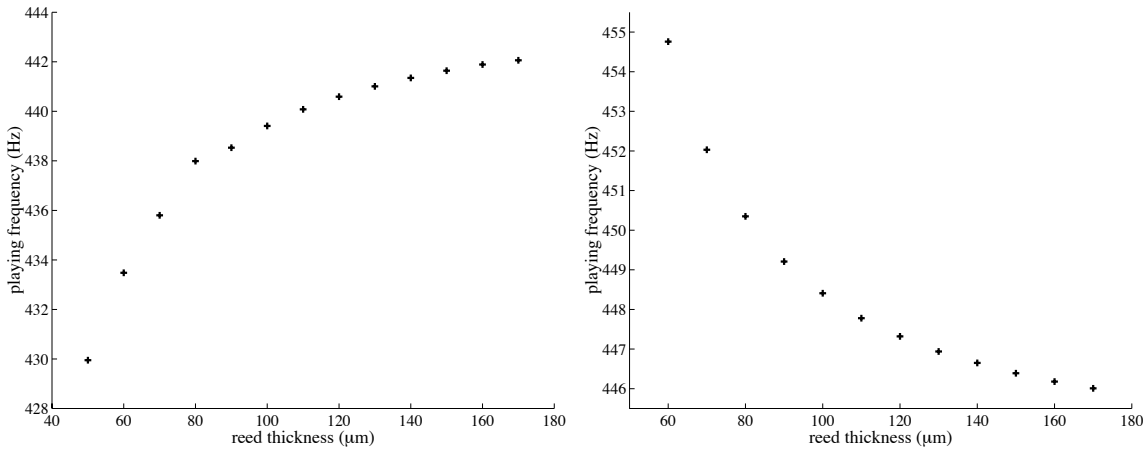

Figure 26: Influence of the variation of e_r, and L_r, over the playing frequency for a (-,+) reed (left) and a (+,-) reed. For a (-,+) reed the playing frequency increases when the reed thickness increases while the playing frequency decreases for a (+,-) reed.

Figure 27 present the variations of the mean, minimum and maximum value of the free tip opening h_n. The mean opening presents strong variations while minimum and maximum present significant ones. The evolutions are almost similar for both reeds and we can notice that there is something like an optimum for the reed opening magnitude where the maximum opening is the biggest and the minimal opening is the tiniest. And this "optimum" thickness configuration corresponds to original reed thickness. We can point out that the magnitude of the reed displacement is about 2 mm which may still correspond to the assumption of a beam with reasonable bending. It is also interesting to note that the mean value is associated with the mean of the minimum and maximum openings which seems normal as the reed motion is quasi sinusoidal.

3.6.2 Case of varying reed width W_r

On figure 28 we plot the evolution of the mean, minimum and maximum over-pressure as a function of the reed thickness but, now, with a variable reed width to keep the reed

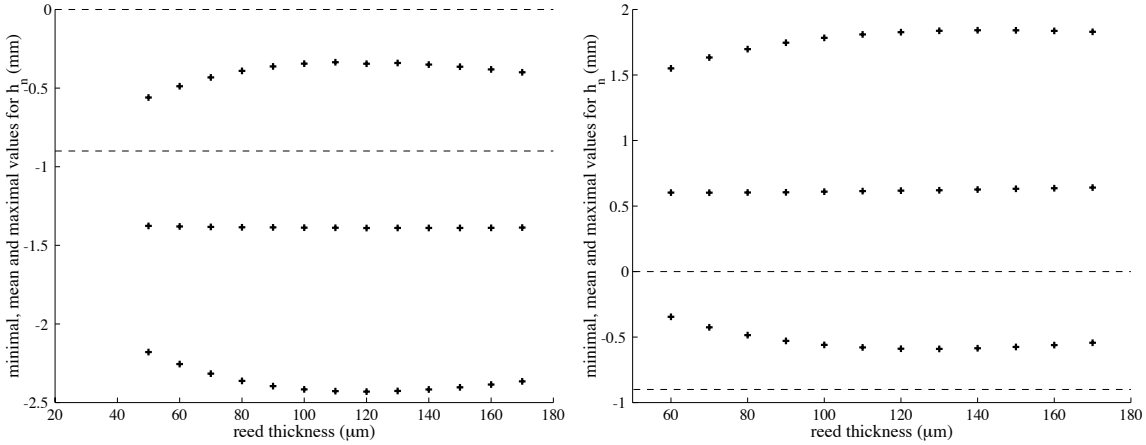

Figure 27: Influence of the variation of e_r, and L_r, over the tip reed opening h_n for a (-,+) reed (left) and a (+,-) reed. The values for the minimum, mean and maximum over-pressure are systematically plotted.

mass constant. Compared to the reed length variable case, while we find a similar plot for the (-,+) reed, the characteristics for the (+,-) have changed: the maximum over-pressure decreases with the increase of the reed thickness; the minimum over-pressure grows and then decreases a little, the mean over-pressure decreases up to a minimum and then increases. But we still find the fact that the mean over-pressure is quite closed to the minimum one so that the mean over-pressure is not representative.

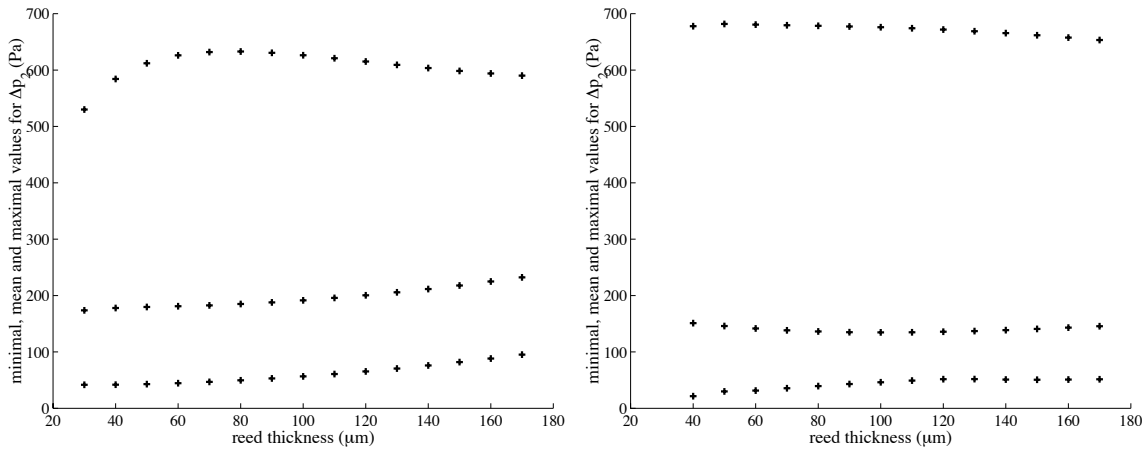

Figure 28: Influence of the variation of e_r, and W_r, over the over-pressure Δp_2 for a (-,+) reed (left) and a (+,-) reed. The values for the minimum, mean and maximum over-pressure are systematicaly plotted.

With Figure 29 we access the characteristic of the playing frequency. We can then notice that the global behaviour for both reeds is quite similar to the one found for the case where the reed length is variable. We still have an increasing playing frequency for the

(-,+) reed, a decreasing playing frequency for the (+,-) reed and a magnitude of variation larger for the (-,+) reed than for the (+,-) reed. Moreover, the playing frequency still remains lower than the reed eigen frequency for the (-,+) reed and higher for the (+,-) reed.

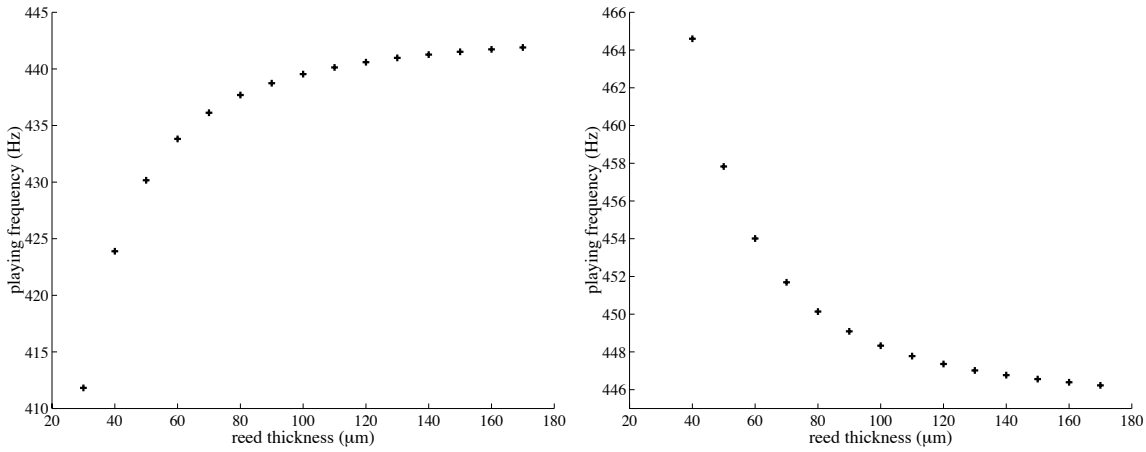

Figure 29: Influence of the variation of e_r, and W_r, over the playing frequency for a (-,+) reed (left) and a (+,-) reed.

Plots of the mean, minimum and maximum free tip openings h_n on Figure 30 exhibit the same behaviour as the one found for the variable reed length: optimum for the opening magnitude closed to the original value of the reed thickness, small variations of the mean opening, mean opening corresponding to the mean of the maximum and minimum openings.

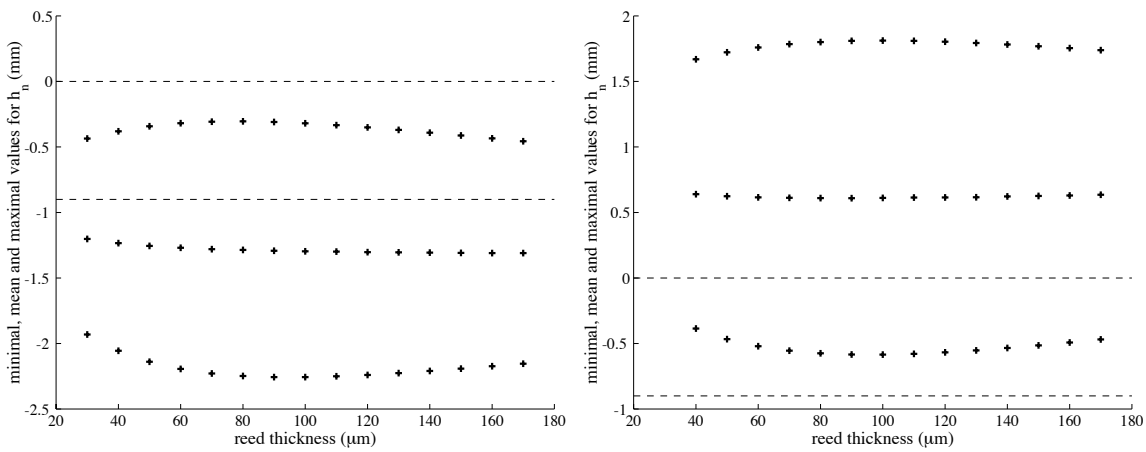

Figure 30: Influence of the variation of e_r, and W_r, over the tip reed opening h_n for a (-,+) reed (left) and a (+,-) reed. The values for the minimum, mean and maximum over-pressure are systematicaly plotted.

With the study of the case where either the reed length or the reed width is variable, we can point out that the reed thickness can have a great influence on the behaviour of the reed. This justifies the need to take into account of the reed thickness in the model of the useful section and to distinguish the neutral, downstream and upstream sections.

4 Conclusion

In this article, we have tried to propose a minimal model for free reeds which may be used to build efficient models for free reed instruments.

We have proposed to introduce corrections into the airflow and above all into the description of the section through which the airflow passes. It seems necessary to take account of the lateral contribution and to define precisely the front contribution. These definitions also need a precise definition of the frontiers of the escape. The reed description and the useful section explicitly introduce the reed thickness. Even if one may think that the reed thickness is too tiny to be taken into account, the study of its influence over the behaviour for both (-,+) and (+,-) reeds shows that its influence is quite important and that we cannot neglect it.

The comparison of numerical simulations derived with three different models of the useful section (Hikichi, Debut and our model) has shown that our model has not the same dynamic behaviour: the reed response is faster and stronger. This result has been found for an artificial triplet excitation and also for a real time-varying one. We also have discussed the needed equations and the validity of their assumptions.

To be able to get some instabilities of both kinds of reeds, we have found that we must introduce a volume and a pipe at the upstream of the reed, on the basis of a linear analysis of the instability conditions. The temporal simulations seem to confirm the qualitative insight given by the instability conditions: reducing the upstream volume helps the oscillations of a (+,-) reed but increasing it is necessary for a (-,+) reed. It has also been shown that the playing frequency of both kinds of reeds is nearly independent of the excitation level. The playing frequency of a (-,+) reed is nearly independent of the size of the upstream volume while, for a (+,-) reed, the playing frequency increases when the upstream volume is reduced and the variations of the playing frequency are important. The increase of the magnitude of the over-pressure is a consequence of the increase of the excitation.

Influence of the excitation velocity v_0 over the over-pressure makes us think that free reeds may present inverse bifuractions because we observe a violent departure from rest and we are able to maintain sound production for excitations lower than the threshold one. But, some experiments should be done to confirm or refute this hypothesis.

We think it is now possible to use this minimal model in the case of free reed instruments such as harmonica, accordeon, harmonium or sho. The application to the case of the harmonica is on the way and the first results of the temporal simulations, to be present elsewhere, are quite promissing. But, there is a great need for experiments with artificial players for all free reeds instruments to be able to validate the models and the associated temporal simulations. It would also be interesting to study the nature of the airflow through the reeds with some more visualisations to improve its description. A discussion on the necessity to use a 3D model of the airflow may also be useful to decide if our model is sufficient not only for high quality synthesis but to study the real behaviour of the instruments and to see if numerical simulations can have the same status as real experiments.

5 Appendix

5.1 Description of the motion of the sections

In the following, we note $M_n(s)$, $M_{up}(s)$ and $M_{do}(s)$ respectively the points of the reed which are on the neutral section, on the upstream and downstream sections of the reed at a distance $s.L_r$ ($s \in [0,1]$, L_r is the reed length) from the clamped end of the reed. We recall that the upstream and downstream sections respectively face the inside and the outside of the instrument. The reference point $O(0,0,0)$ is taken at the clamped end, on the middle of the width and on the downstream side of the support (outside of the instrument) as illustrated by figure 31 for a (-,+) and a (+,-) reed.

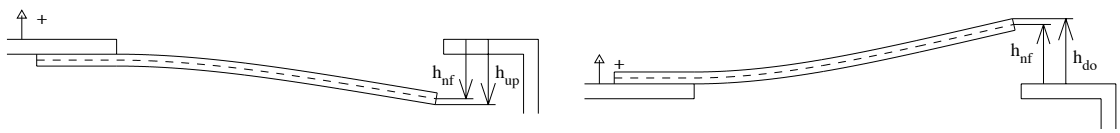

Figure 31: (left) Illustration of the convention chosen for the transverse displacements $h_n(s)$ and $h_{up}(s)$ of the neutral and downstream sections in the case of a (-,+) reed. (right) Illustration of the convention for the transverse displacement $h_{do}(s)$ of the downstream section in the case of a (-,+) reed. These displacements are used to calculate the useful sections.

As we assume the reed to vibrate on its first transverse eigen mode and we note h_n and $h_{n,000}$ the current and plane transverse position of the neutral section, the local neutral section point $M_n(s)$ coordinates are $(x_n(s), 0, h_n(s))$ (point situated on the middle of the width of the reed) where:

$$x_n(s) = s.Lr$$

and

$$h_n(s) = h_{n,000} + (h_n - h_{n,000})\psi(s)$$

where $\psi(s)$ is the normalised modal reed factor for the first transverse eigen mode.

Considering the figure 31, we can observe that when the reed is plane, the transverse positions $h_{n,000}$ of the (-,+) and (+,-) reeds are different:

- $h_{n,000} = -e_s - \dfrac{e_r}{2}$ for a (-,+) reed;
- $h_{n,000} = \dfrac{e_r}{2}$ for a (+,-) reed

where e_r and e_s are the reed and support thickness.

In these conditions, the coordinates of the normal $\overrightarrow{n(s)}$ to neutral section, at distance $s.L_r$ from the clamped end, are:

$$\overrightarrow{n(s)} = \begin{pmatrix} \dfrac{-(h_n - h_{n,000})\psi'(s)}{\sqrt{L_r^2 + (h_n - h_{n,000})^2\psi'(s)^2}} \\ 0 \\ \\ \dfrac{L_r}{\sqrt{L_r^2 + (h_n - h_{n,000})^2\psi'(s)^2}} \end{pmatrix}$$

The points $M_{up}(s)$ and $M_{do}(s)$ of the upstream and downstream sections associated with the point $M_n(s)$ of the neutral section are then given by:

$$\overrightarrow{OM_{up}(s)} = \overrightarrow{OM_n(s)} - \frac{e_r}{2}\overrightarrow{n(s)}$$

and

$$\overrightarrow{OM_{do}(s)} = \overrightarrow{OM_n(s)} + \frac{e_r}{2}\overrightarrow{n(s)}$$

So we have, for $x_{up}(s)$, $h_{up}(s)$, $x_{do}(s)$ and $h_{do}(s)$:

- $x_{up}(s) = s.Lr + \dfrac{e_r}{2}\dfrac{(h_n - h_{n,000})\psi'(s)}{\sqrt{L_r^2 + (h_n - h_{n,000})^2\psi'^2(s)}}$;
- $h_{up}(s) = h_n(s) - \dfrac{e_r}{2}\dfrac{L_r}{\sqrt{L_r^2 + (h_n - h_{n,000})^2\psi'^2(s)}}$;
- $x_{do}(s) = s.Lr - \dfrac{e_r}{2}\dfrac{(h_n - h_{n,000})\psi'(s)}{\sqrt{L_r^2 + (h_n - h_{n,000})^2\psi'^2(s)}}$;
- $h_{do}(s) = h_n(s) + \dfrac{e_r}{2}\dfrac{L_r}{\sqrt{L_r^2 + (h_n - h_{n,000})^2\psi'^2(s)}}$.

We introduce the following quantities to simplify the expressions:

- $\Delta x_{up}(s) = x_{up}(s) - s.L_r$ which corresponds to the longitudinal displacement of the upstream section;
- $\Delta x_{do}(s) = x_{do}(s) - s.L_r$ which corresponds to the longitudinal displacement of the downstream section.

5.2 Reed motion equation and pumped flow

In the case of free reeds, we have already seen that the reed motion corresponds to the first transverse eigenmode of a clamped-free beam so we can write the local transverse deformation $\xi(s,t) = \psi(s).\zeta(t)$ (of the neutral section at a distance $s.L_r$ from the clamped end) with $\zeta(t) = h_n(t) - h_{n,00}$ where $h_{n,00}$ is the unblown tip opening of the neutral section of the reed.

For the neutral section, the reed motion equation is classically given by

$$\frac{d^2\zeta}{dt^2} + Q^{-1}\omega_0\frac{d\zeta}{dt} + \omega_0^2\zeta = \mu\Delta p \tag{11}$$

where :

- Q and ω_0 are directly determined by calibration ;
- $\mu = \dfrac{S_r}{M}$ with $S_r = W_r\displaystyle\int_0^{L_r}\psi(s)ds$ and M given by $M = \dfrac{K}{\omega_0^2}$ as calibration gives the stiffness K rather than M.

We also have to introduce the equation of the pumped flow. This flow can be defined by an equivalent expression $u_p = S_p\dfrac{d\zeta}{dt}$ or by a local expression $u_p = W_r\displaystyle\int_0^{L_r}\frac{\partial\xi(s,t)}{\partial t}ds$. As we have $\xi(s,t) = \psi(s).\zeta(t)$, we find after some calculation that:

$$S_p = S_r = W_r\int_0^{L_r}\psi(s)ds \tag{12}$$

We do not distinguish S_p and S_r in practice and only use S_r in case of free reeds instruments.

5.3 Derivation of the conditions for instabilities

Given the symmetry of the laws for the useful section, $S_u = S_{u00} + a_1\zeta^2$ is a fair approximation of the useful section near the mean opening. In the following, we note $\zeta_0 = h_{n,0} - h_{n,00}$ where $h_{n,0}$ is the mean opening, $\zeta_{00} = h_{n,00} - h_{n,000}$ and $S_{u0} = S_{u00} + a1(\zeta_0 - \zeta_{00})^2$. We also use the prime suffix for the variable or acoustical part of quantities used in the calculation: ζ' is for instance the acoustical part of ζ while ζ_0 is the mean value of ζ.

The Fourier transforms are noted using capital letters and are associated with the angular frequency ω: p_2' has $P_2'(\omega)$ for Fourier transform ; ζ' is an exception because its Fourier transform is written $\zeta'(\omega)$. We also need to introduce the useful quantity $A = 2a_1(\zeta_0 - \zeta_{00})v_{j0}$.

To derive the condition for the instabilities of both (-,+) and (+,-) reeds, we first need to linearise the equations and then calculate the Fourier transform of the linearised equations. We then get the following set of equations :

- $\dfrac{V_1}{c_0^2}\dfrac{d(p_1 - p_{atm})}{dt} = \rho_0(u_0 - u)$ gives $\mathrm{j}\omega\dfrac{V_1}{c_0^2}P_1'(\omega) = -\rho_0.U'(\omega)$ (L1);
- $p_1 = p_2 + \rho_0\dfrac{L_2}{S_2}\dfrac{du}{dt}$ becomes $P_1'(\omega) = P_2'(\omega) + \mathrm{j}\omega\rho_0\dfrac{L_2}{S_2}U'(\omega)$ (L2);
- $p_2 = p_{atm} + \dfrac{1}{2}\rho_0 v_j^2$ gives $V_j'(\omega) = \dfrac{P_2'(\omega)}{\rho_0.v_{j0}}$ (L3) ;
- $\dfrac{d^2\zeta}{dt^2} + Q^{-1}\omega_0\dfrac{d\zeta}{dt} + \omega_0^2\zeta = \mu(p_2 - p_{atm})$ becomes $(-\omega^2 + \mathrm{j}\omega Q^{-1}\omega_0 + \omega_0^2)\zeta'(\omega) = \mu P_2'(\omega)$ (L4) ;
- $u = S_r\dfrac{d\zeta}{dt} + \alpha S_u v_j$ gives $U'(\omega) = \mathrm{j}\omega S_r\zeta'(\omega) + \alpha S_u V_j'(\omega) + \alpha A\zeta'(\omega)$ (L5)

We can then introduce the expression of $P_1'(\omega)$ using equation (L2) and of $U'(\omega)$ using equation (L5) in the mass conservation (L1) which gives, when replacing $V_j'(\omega)$ by its expression as a function of $P_2'(\omega)$ using (L3):

$$\begin{aligned}\mathrm{j}\omega\frac{V_1}{c_0^2}\big[P_2'(\omega) + \mathrm{j}\omega\rho_0\frac{L_2}{S_2}\big(\mathrm{j}\omega S_r\zeta'(\omega) + \frac{\alpha S_{u0}}{\rho_0 v_{j0}}P_2'(\omega) + \alpha A\zeta'(\omega)\big)\big]\\ = \mathrm{j}\omega S_r\zeta'(\omega) + \frac{\alpha S_{u0}}{\rho_0 v_{j0}}P_2'(\omega) + \alpha A\zeta'(\omega - \rho_0\big[\mathrm{j}\omega S_r\zeta'(\omega) + \frac{\alpha S_{u0}}{\rho_0 v_{j0}}P_2'(\omega) + \alpha A\zeta'(\omega\big]\end{aligned}$$

which can also be written, after some calculation, as

$$\begin{aligned}P_2'(\omega) = \frac{-\rho_0\big(1 - \frac{V_1 L_2}{c_0^2 S_2}\omega^2\big)}{\big(\frac{\alpha S_{u0}}{v_{j0}}\big)^2\big(1 - \frac{V_1 L_2}{c_0^2 S_2}\omega^2\big)^2 + \big(\frac{V_1}{c_0^2}\omega\big)^2}.\Bigg[\alpha A\frac{\alpha S_{u0}}{v_{j0}}\big(1 - \frac{V_1 L_2}{c_0^2 S_2}\omega^2\big) + \omega^2 S_r\frac{V_1}{c_0^2}\\ + \mathrm{j}\omega\bigg(S_r\frac{\alpha S_{u0}}{v_{j0}}\big(1 - \frac{V_1 L_2}{c_0^2 S_2}\omega^2\big) - \alpha A\frac{V_1}{c_0^2}\bigg)\Bigg].\zeta'(\omega)\end{aligned}$$

The instability of the reed should be possible if the damping term in (L4), $\mathrm{j}\omega Q^{-1}\omega_0\zeta'(\omega)$ is at least compensated by the part of $P_2'(\omega)$ associated with $\mathrm{j}\omega P_2'(\omega)$. In such condition, we must verify :

$$Q^{-1}\omega_0 < -\mu\rho_0\big(1-\frac{V_1L_2}{c_0^2S_2}\omega^2\big)\frac{S_r\frac{\alpha S_{u0}}{v_{j0}}\big(1-\frac{V_1L_2}{c_0^2S}\omega^2\big)-\alpha A\frac{V_2}{c_0^2}}{\big(\frac{\alpha S_{u0}}{v_{j0}}\big)^2\big(1-\frac{V_1L_2}{c_0^2S_2}\omega^2\big)^2+\big(\frac{V_1}{c_0^2}\omega\big)^2}$$

which can only be fullfilled if we have

$$\left(1-\frac{V_1L_2}{c_0^2S_2}\omega^2\right).\left[S_r\frac{\alpha S_{u0}}{v_{j0}}\big(1-\frac{V_1L_2}{c_0^2S}\omega^2\big)-\alpha A\frac{V_2}{c_0^2}\right]<0$$

As $A>0$ for a (+,-) reed, $1-\dfrac{V_1L_2}{c_0^2S_2}\omega^2>0$ must be fullfilled to get potential instabilities while, as $A<0$ for a (-,+) reed, it is $1-\dfrac{V_1L_2}{c_0^2S_2}\omega^2<0$ which must be verified.

5.4 Keypoints of the numerical simulations method

To perform numerical simulations with these models of free reeds, we have followed the method proposed by Gazengel *et al* in [14] to derive the numerical equivalents for the models so we invite the reader to consult the article of Gazengel for full details: we only give the keypoints of the numerical algorithm.

Except for the reed motion equation, the numerical equivalents are derived with replacement of derivatives using the backward Euler numerical scheme.

The numerical equivalent for the reed motion equation is derived using a bilinear transform, with pre-dilatation of the frequency ω_0 as proposed by Gazengel [14] and the introduction of the pumped flow to replace a second-order differential equation by a system of two first-order differential equations.

To calculate the signals for sample n we assume that the over-pressure $\Delta p_2[n]$ equals the $\Delta p_2[n-1]$ and considering $\Delta p_2[n]$ we express all the other quantities ($\zeta_n[n]$, $v_j[n]$, $S_u[n]$, $u_p[n]$, $u_t[n]$, $u[n]$ and $\Delta p_1[n]$) as functions of $\Delta p_2[n]$. The main, non linear equation to solve corresponds to the numerical version of the mass conservation for volume V_1:

$$NL\big[\Delta p_2[n]\big]=\frac{V_1}{\rho_0c_0^2}F_s\big(\Delta p_1[n]-\Delta p_1[n-1]\big)-u_0[n]-u[n]$$

where F_s is the sampling frequency.

Using the Newton-Raphson scheme, we calculate the new value of $\Delta p_2[n]$, which would be closest to the wanted value, as :

$$\Delta p_2[n]\ \mapsto \Delta p_2[n]-\frac{1}{NL\big[\Delta p_2[n]\big]}.\frac{d}{d\Delta p_2[n]}\Big(NL\big[\Delta p_2[n]\big]\Big)$$

We keep on calculate new values of $\Delta p_2[n]$ until the variation is lower than the chosen precision. When this value of $\Delta p_2[n]$ is finally found we calculate the other quantities and begin the calculation of the next sample ($\Delta p_2[n+1]$).

As proposed by Gazengel, we always verify if the corrections for the $\Delta p_2[n]$ make sense, that is to say if the correction does not correspond to oscillations around the wanted value. If we note that the algorithm is oscillating around the solution we then adopt a dichotomy scheme to calculate the good approximation of $\Delta p_2[n]$.

As previously indicated, we pre-calculate tables for the useful section and its derivative $dS_u/d\Delta p_2$ to increase the velocity of the calculation.

At the beginning of the calculation we know the whole excitation signal and suppose that the reed is at rest.

We must emphasise that we calculate all the quantities with the asumption of an acoustical flow. Indeed, we do not distinguish a mean flow and acoustical pertubations as mean quantities do not seem to make sense for the configurations we have studied.

References

[1] H. von Helmhotz. App. VII, In the theory of pipes. In Dover, editor, *On The Sensations Of Tone*, page 576. Dover Publications, Inc., New York, second english edition, 1954.

[2] T. A. Wilson and G. S. Beavers. Operating modes of the clarinet. *J. Acoust. Soc. Am.*, 56(2):653–658, 1974.

[3] C. J. Nederveen. *Acoustical Aspects of Woodwind Instruments.* Nothern Illinois University Press, Dekalb, 1998.

[4] J. Saneyoshi, H. Teramura, and S. Yoshikawa. Feedback Oscillations in Reed Woodwind and Brasswind Instruments. *Acustica*, 62(3):194–210, 1987.

[5] N. Grand, J. Gilbert, and F. Laloe. Oscillation threshold of woodwind instruments. *Acustica*, 82:137–151, 1996.

[6] J. Kergomard. Elementary considerations on reed-instrument oscillations. In A. Hirschberg/ J. Kergomard/ G. Weinreich, editor, *Mechanics of musical instruments*, volume 335 of *CISM Courses and Lectures*, pages 229–290. Springler-Verlag, Wien-New York, 1995.

[7] J.-P. Dalmont, J. Gilbert, and J. Kergomard. Reed instruments, from Small to Large Amplitude Periodic Oscillations and the Helmholtz Motion Analogy. *Acta Acustica*, 86:671–684, 2000.

[8] J. Kergomard, Ollivier S., and Gilbert J. Calculation of the Spectrum of Self-Sustained Oscillators Using a variable Truncation Method: Application to Cylindrical Reed Instruments. *Acta Acustica*, 86:685–703, 2000.

[9] S. Ollivier, J.-P. Dalmont, and J. Kergomard. Idealized Models of Reed Woodwinds. Part I: Analogy with the bowed string. *Acta Acustica united with Acustica*, 90:1192–1203, 2004.

[10] S. Ollivier, J.-P. Dalmont, and J. Kergomard. Idealized Models of Reed Woodwinds. Part II: On the stability of "two-step" oscillations". *Acta Acustica united with Acustica*, 91:166–196, 2005.

[11] R. T. Schumacher. Self-sustained oscillations of the clarinet: an integral approach. *Acustica*, 40:298–309, 1978.

[12] R. T. Schumacher. Ab Initio Calculations of the Oscillations of a Clarinet. *Acustica*, 48(2):71–85, 1981.

[13] M. E. McIntyre, R. T. Schumacher, and J. Woodhouse. On the oscillations of musical instruments. *J. Acoust. Soc. Am.*, 74(5):1325–1345, 1983.

[14] B. Gazengel, J. Gilbert, and N. Amir. Time domain simulation of single reed wind instrument. From the measured input impedance to the synthesis signal. Where are the traps ? *Acta Acustica*, 3:445–472, 1995.

[15] Ph. D. Koopman and J. P. Cottingham. Acoustical properties of free reeds. *Reed Organ Society Bulletin*, 15(3):17–23, 1997.

[16] H. T. Bahnson, J. F. Antaki, and Q. C. Beery. Acoustical and physical dynamics of the diatonic harmonica. *J. Acoust. Soc. Am.*, 103(4):2134–2144, 1998.

[17] J. P. Cottingham, C. H. Reed, and M. Busha. Variation of frequency with blowing pressure for an air-driven free reed. In DEGA, editor, *Forum Acusticum*, Berlin, 1999.

[18] J. P. Cottingham, J. C. Lilly, and C. H. Reed. The motion of air-driven free reeds. In DEGA, editor, *Forum Acusticum*, Berlin, 1999.

[19] J. P. Cottingham. Pitch bending and anomalous behaviour in a free coupled to a pipe resonator. *Acta Acustica united with Acustica*, 91 (Suppl. 1):S47, 2005.

[20] V. K. Singhal. *Acoustics of ducts with flow and its relation to acoustically induced valve-pipe instabilities*. PhD thesis, Massachussets Institute of technology (MIT), 1976.

[21] N. H. Fletcher. Excitation Mechanisms in Woodwind and Brass Instruments. *Acustica*, 43:63–72, 1979.

[22] N. H. Fletcher. Air flow and sound generation in musical wind instruments. *Ann. Rev. Fluid Mech.*, 11:123–146, 1979.

[23] N. H. Fletcher, R. K. Silk, and L. M. Douglas. Acoustic Admittance of Air-Driven Reed Generators. *Acustica*, 50:155–159, 1982.

[24] R. Johnston. Pitch Control in Harmonica Playing. *Acoustics Australia*, 15(3):69–75, 1987.

[25] N. H. Fletcher. Autonomous vibration of simple pressure-controlled valves in gas flow. *J. Acoust. Soc. Am.*, 93(4):2172–2180, 1993.

[26] C. Cuesta and C. Valette. Playing chromatically on a diatonic harmonica: an investigation of the mechanisms. In *Proc. Int. Symp. Mus. Acoust.*, pages 107–113, Dourdan, 1995. IRCAM.

[27] N. H. Fletcher and A. Tarnopolsky. Acoustics of the avian vocal tract. *J. Acoust. Soc. Am.*, 105(1):35–49, 1999.

[28] A. Z. Tarnopolsky, Fletcher N. H., and Lai J. C. S. Oscillating reed valves- An experimental study. *J. Acoust. Soc. Am.*, 101:400–406, 2000.

[29] N. H. Fletcher and T. D. Rossing. *The Physics of Musical Instruments.* Springer-Verlag, New-York, 2000.

[30] A. O. St Hilaire, T. A. Wilson, and G. S. Beavers. Aerodynamic excitation of the Harmonium reed. *J. Fluid Mech.*, 49:803–818, 1971.

[31] R. R. Van Hassel and A. Hirschberg. Comments on Linear Theory of Harmonium Reed Oscillation. In *ISMA'95*, pages 130–133, Dourdan (France), 1995. SFA.

[32] N. Misdariis, D. Ricot, and R. Cossé. Modélisation physique de la vibration d'une anche d'accordéon. In *Proceedings of the 5th French Congress on Acoustics (CFA 2000)*, pages 281–284, Lausanne (Switzerland), 2000. Presses Polytechniques et Universitaires Romandes.

[33] R. R. Van Hassel and A. Hirschberg. Linear theory of harmonium reed oscillation. In *International Symposium on Musical Acustics (ISMA 2001)*, Perugia (Italy), 2001. Catgut society.

[34] L. Millot. *Étude des instabilités des valves : application à l'harmonica diatonique.* PhD thesis, Université Paris 6, 1999.

[35] L. Millot, C. Cuesta, and C. Valette. Experimental results when playing chromatically on a diatonic harmonica. *Acta Acustica*, 87:262–270, 2001.

[36] D. Ricot. Modélisation physique de la vibration d'une anche d'accordéon- application à la synthèse sonore. DEA report, IRCAM, August 1999.

[37] J. Backus. Small-vibration theory of the clarinet. *J. Acoust. Soc. Am.*, 35(3):305–313, 1963.

[38] S. C. Thompson. The effect of the reed resonance on woodwind production. *J. Acoust. Soc. Am.*, 66:1299–1307, 1979.

[39] S. D. Sommerfeldt. Ab Simulation of a player-clarinet system. *J. Acoust. Soc. Am.*, 83(5):1908–1918, 1988.

[40] A. Hirschberg, R. W. A. Van de Laar, J. P. Marrou-Mauriéres, A. P. J. Wijnands, H. J. Dane, S. G. Kruijswijk and A. J. M. Houtsma. A Quasi-stationary Model of Air Flow in the Reed Channel of Single-reed Woodwind Instruments. *Acustica*, 70:146–154, 1990.

[41] A. Hirschberg. Wind instruments (chapter from C.I.S.M. course: Mechanics of Musical Instruments). Vakgroep Transportfysica Report R-1290-D, Eindhoven University of Technology, July 1994.

[42] T. Hikichi and N. Osaka. Time domain simulation of the sound production of the sho, the japanese free-reed mouth organ. In *Proc. Int. Symp. Mus. Acoust.*, pages 71–76, Perugia, 2001. Fondazione Scuola di San Giorgio.

[43] V. Debut and Millot L. Time domain simulation of the diatonic harmonica. In *Proc. Int. Symp. Mus. Acoust.*, pages 51–66, Perugia, 2001. Fondazione Scuola di San Giorgio.

[44] V. Debut and Millot L. Time domain simulation of the diatonic harmonica. In *Workshop on current research direction in computer music : Mosart european program*, pages 143–146, Barcelona, 2001. Audiovisual Institute of the Pompeu Fabra University.

[45] V. Gibiat. private communications, 2002.

[46] B. Fabre and Hirschberg A. From sound synthesis to instrument making: an overview of recent researches on woodwinds. In *Stockholm Music Acoustics Conference*, pages 239–242, Stockholm, 2003. KTH, Department of Speech Music Hearing.

View publication stats